Jyrki Rasku

Classification of the human swaying processes: A machine learning approach

ACADEMIC DISSERTATION

To be presented, with the permission of the Faculty of Information Sciences of the University of Tampere, for public discussion in the Pinni B1096 Auditorium of the University on October 23rd, 2009, at 12 noon.

DEPARTMENT OF COMPUTER SCIENCES
UNIVERSITY OF TAMPERE

A-2009-4

TAMPERE 2009

Supervisor: Prof. Martti Juhola
University of Tampere

Opponent: Prof. Tapio Grönfors
University of Kuopio

Reviewers: Prof. Pekka Loula
Tampere University of Technology, Pori

Prof. Jussi Parkkinen
University of Joensuu

Electronic dissertation
Acta Electronica Universitatis Tamperensis 899
ISBN 978-951-44-7878-9 (pdf)
ISSN 1456-954X
http://acta.uta.fi

Department of Computer Sciences
FIN-33014 UNIVERSITY OF TAMPERE
Finland

ISBN 978-951-44-7856-7
ISSN 1459-6903

Tampereen yliopistopaino Oy
Tampere 2009

Abstract

According to Central Statistical Office of Finland falls are a more common cause of death in Finland than ground traffic accidents. Furthermore, hip fractures caused by falls among the oldest old are usually impossible to cure properly; they are expensive and cause reduction in the quality of life. Against this background a method for predicting the risk of falling is needed. Furthermore, suitable methods for improving the weakened ability to maintain balance should be studied. In this work the focus is on the classification of measured human swaying data. The classification of swaying data can be considered as a starting point of the prediction of increased risk of falling.

The evaluation of human ability to maintain balance is primarily done by analyzing the results of Computerized Dynamic Posturography (CDP). During CDP a subject is standing on the force platform which records his/her body movements originated from the muscle activity required to keep the upright stance. Analyzing the results of CDP is diverse and there is no single best method known.

In this work machine learning methods such as hidden Markov models are applied to CDP data which was measured from students, otoneurological patients and elderly subjects. The primary goal is in the prediction of the origin of unknown CDP data. For instance, is unknown data measured from a young student or from an otoneurological patient? In certain cases this prediction can be used as an indicator that a preventive action should be taken. For instance, if a young person's swaying data resembles the data of an elderly, there might be something wrong in his or her postural control system.

Depending on the study in question (students, patients and elderly) the correct prediction accuracies in this work varied between 65-90%. This result is good, because the visual discrimination of swaying data is very difficult and differences between subject classes are subtle. For instance, if there are two graphs from signals which are measured from different swaying processes, it is almost impossible to say the origin of the signals with visual inspection.

Keywords: Hidden Markov Models, Postural Control, Classification.

Acknowledgements

Accomplishing of this work has been extremely challenging. Fortunately, I have managed to get support from individuals who have had expertise in many fields. First of all, I want to thank my supervising professor Martti Juhola who has been a patient, encouraging and good boss. I am also grateful to professor Jyrki Nummenmaa, the head of the Department of Computer Sciences, about arranging a pleasant working environment.

Special thanks go to professor Ilmari Pyykkö who has provided the medical expertise, patients and elderly subjects for this research. I also want to express my gratitude to docent Esko Toppila and Timo Tossavainen, Ph.D, for technical guidance concerning measuring devices and software interfaces. In addition, I want to thank Eeva Tuunainen for measuring the elderly subjects.

I am extremely grateful to Arto Luoma, Ph.D, professor Erkki Liski and Simo Puntanen, Ph.D who have helped me to fill the gap of the statistical whole in my head.

I want to thank the Academy of Finland and Oskar Öflund Stiftelse for financial support.

The support from my family has been very important, so I want to thank my wife Petra, my son Tuukka and my daughter Elli.

Last but not least, I thank my peer support group for valuable conversations. This group contains Pekka Niemenlehto, Kirsi Varpa and the rest of DARG personnel.

Contents

1 Introduction 1
2 Human balance system 2
3 Diagnostic tests and decision support 3
4 Data collection 5
4.1 Equipment 5
4.2 Data 8
5 Features 10
5.1 System Identification and linear digital filtering 10
5.2 Dimension reduction 12
6 Machine learning and methods applied 14
6.1 Hidden Markov models 15
6.2 Discrete Kalman filters 16
6.3 Neural networks 17
6.4 Fisher's linear discriminant 18
6.5 *k*-nearest neighbour 20
6.6 Mahalanobis distance 21
7 Performance of a classifier 23
8 Results 24
8.1 Publication 1 25
8.2 Publication 2 26
8.3 Publication 3 26
8.4 Publication 4 27
8.5 Publication 5 28
9 Discussion 29
10 Conclusion 30
11 Personal contributions 32
12 References 33

List of abbreviations

AD	Analog Digital
ANN	Artificial Neural Network
AR	Autoregressive Model
ARX	Autoregressive Exogenous Model
CDP	Computerized Dynamic Posturography
COP	Centre of Pressure
ENG	Electronystagmography
HMD	Head Mounted Display
HMM	Hidden Markov Model
KNN	*k*-Nearest Neighbour
ONE	Otoneurological Expert System
PCA	Principal Component Analysis
VOR	Vestibulo-Ocular Reflex

List of the original publications

1. J. Rasku, M. Juhola, T. Tossavainen, I. Pyykkö, E. Toppila, Modelling Stabilograms with hidden Markov models, *Journal of Medical Engineering & Techonology*, 32(4), pp. 273-283, 2008.
2. J. Rasku, M. Juhola, E. Toppila, I. Pyykkö, Recognition of balance signals between healthy and otoneurological patients with hidden Markov models, *Biomedical Signal Processing and Control*, 2(1), pp. 1-8, 2007.
3. J. Rasku, M. Juhola, A detection method of body movement signals measured with magnetic tracking device for human balance investigations, to appear in *International Journal of Medical Engineering and Informatics.*
4. J. Rasku, M. Juhola, Looking for differences in postural control systems: young students versus pensioners, *6th IASTED International Conference on Biomedical Engineering*, pp. 108-112, Innsbruck, 2008.
5. J. Rasku. A method for the classification of corrective activity in context dependent postural controlling tasks. *Computers in Biology and Medicine* 39(10), pp. 940-945, 2009.

1 Introduction

A healthy human being finds it easy to walk, run and ride a bike. With additional physical training he or she may be able to perform demanding balance related tasks. For instance, jumps in figure skating and snowboarding can become entirely automatic after thousands of repetitions. Usually this is the case and it indicates that a person's postural control system is working properly.

Unfortunately, the ability to maintain balance can weaken because of different reasons. It is known that older people tend to fall down quite often. As a matter of fact, several of them suffer from the fear of falling [87] because they are aware of their poor balance control ability. This can lead to a situation where an individual begins to avoid walking and this way accelerates the weakening of his or her physical condition. In this case there is an increased risk of social isolation and the reduction in the quality of life. In addition to elderly, reduced ability to maintain the upright stance straddles among people who have greatly been affected by noise [50, 74] or solvents [84].

Aging, noise and solvents among other environmental factors affect the human postural control system. It is an open question what this affecting mechanism is. Because the nature of the human postural control system is very complex, the collaboration between physicians, computer scientists and physicists is necessary.

In this collaboration the role of physicians is to analyze medicals interests of the work and to define the problem and what tools are needed to accomplish the goal. The planning and implementation of tools are the task of physicists. To provide reasonable methods and results for the use of physicians is the work of computer scientists.

At its best, the collaboration can produce an implementation and use of an expert system which can support physicians in reliable and consistent diagnosis making. Because the implementation of such an expert system is a difficult and time consuming task, it should be divided into several small parts which are possible to implement independently of each other. A gradual integration of these parts will eventually produce a functional system. The purpose of this thesis is to propose a set of features and machine learning methods which can extract information of human swaying process. Considering these features and methods can be thought as the first iteration of the implementation of an expert system. In this thesis the way to approach the problem is purely data driven.

Previous balance research has primarily focused on validating the measurement procedures [23, 56], studying the effects of certain predefined tasks [14, 18], biomechanical modeling [34, 88] and system identification [15, 21, 51]. In this thesis the point of view is in the classification of different human swaying patterns. According to knowledge of the author, this sort of research has not been done previously.

The purpose of the introductory part is to give the necessary background information for a reader to read through the articles attached after Section 12. Section 2 depicts the internal structure of the human postural control system researched. In Section 3 a short introduction of research methods of the balance system is presented and the purpose of an expert system is outlined. Section 4 deals with the data collection procedure, which was the starting point of this work. In Section 5 the main interest is

to explore how to extract interesting information out of the collected data. Also, the concepts of system identification and linear digital filtering are presented. The aim of Section 6 is to clarify the machine learning and pattern recognition methods. In Section 7 the usefulness of a trained computer classifier is addressed. Section 8 summarizes the ideas and results presented in the original articles of the thesis. The purpose of Section 9 is to discuss the research made and the results gained. Finally Section 10 gives the conclusion.

2 Human balance system

In order to maintain balance human beings need to know their relative position and orientation in the surrounding world. This information comes from three different channels, which are the eyes, the vestibular organs in the inner ears and the somatosensory receptors in muscles [4, 24].

Information flows to the brain stem where it is integrated and combined to the learned information patterns. There is a repertoire of learned patterns. For instance, a human being uses different strategies when walking on a slippery or normal platform [32]. Sometimes information from the different channels can be contradictory. An example of this situation is a moving train. A person can stand in a stationary train while another train slowly passes by. The visual information of a moving train can create an illusion that the person is actually moving. However, the feedback from somatosensory system rapidly corrects the wrong visual information.

After the integration of information the brain sends motor commands to the eyes and muscles which cause the repositioning of the body to a more stable state. Getting information from the environment and making the corrective actions is a continuous loop which is depicted in Figure 1.1.

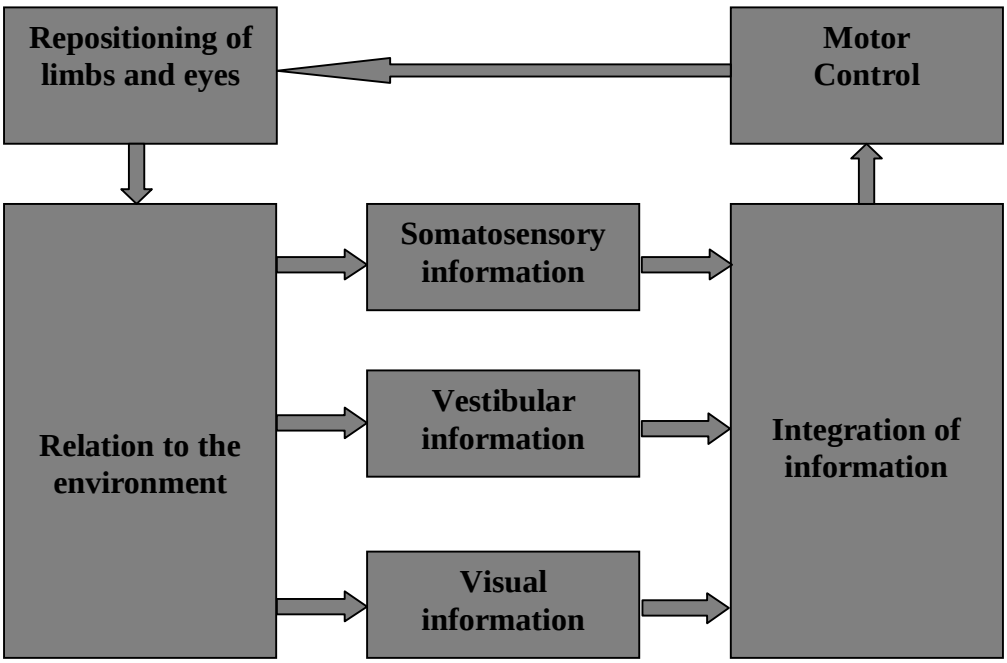

Figure1.1: The human balance system

The vestibular organs and the eyes are closely connected [5]. When a person turns the head, the vestibular organs signal the eyes to turn in the opposite direction to keep the gaze at the same target [44, 52]. This mechanism makes the clear vision possible and it is called the vestibulo-ocular reflex (VOR). This reflex can be verified easily. If a person reads a paper and moves the head up and down or to left and right the reading is possible. However, if a person keeps the head still and moves the paper by the arms reading becomes impossible. The clear image formation in the brain is possible only when the eyes do not move largely in the relation to the environment. The image from the surrounding world is ultimately created in the brain. However, the input data for the image is a set of photons from the environment which are captured by the rods and cones inside the eyes. The rods and cones [29] react differently for photons with varying energy. This energy can also be considered as electromagnetic radiation with different frequencies, which represent all colours in the visible band of the electromagnetic spectrum [26]. When the rods and cones have reached a steady state under the electromagnetic excitation, the image is formed in the brain. The function of a vestibular organ is based on the inertia. In both ears there are three semicircular canals which are perpendicular to each other. These canals contain liquid which lags behind when the head is turned. This lag is perceived as an angular acceleration which is converted to orientation information in the brain [5].

The somatosensory information from muscles tells how the limbs are positioned and also the force feedback from the ground under the feet. This information makes the fast correction actions possible, for instance, when walking in the woods. An individual can test the effect of limited somatosensory information by walking on a thick foam mattress.

3 Diagnostic tests and decision support

Because the human postural system is complex, there is no single test which could reveal the reason for impaired balance. However, there are tests which can tell the state of the co-operation of the vestibular organs, the brain stem and the eyes.

In many cases a patient with balance deficits also suffers from hearing loss. This is natural because the hearing and vestibular organs are closely related [66]. In this case basic auditory tests [46] can give a hint about a problem in the inner ear.

As stated previously, the vestibular organs and the eyes work together. If there is a problem in this co-operation, the culprit can be the vestibular organ or the brain stem. The co-operation can be tested with electronystagmography (ENG) [5, 6] and rotation tests [25] The drawback in this approach is that ENG only tells if the pathways in the inner ear and nervous system are functioning normally. The state of individual organs must be inferred by using a patient's medical history and symptoms.

Nowadays ENG is performed with infrared cameras which are connected to a computer. The purpose of the infrared cameras is to record eye movements during testing in a dimmed room. The computer stores the image data for later analysis. An ENG test battery consists of three main phases. In the first phase of a test a subject sits on a chair and stares a tiny stationary red light on the wall. The purpose of this phase is to test whether pathologic nystagmus is present or not. Nystagmus is an unintended eye movement where the eyes move back and forth. In a small extent this is normal, but large movements can cause dizziness. After this phase the red light moves

horizontally to the left and then to the right and the computer records the eye movements. In this test the subject is instructed to follow the moving red light only with his/her eyes while the orientation and rotation of head remain unchanged. This effectively tests the subject's visual-ocular control. Deficits in visual-ocular control can cause difficulties in maintaining balance, because clear image formation from the environment is more difficult than in a situation where the visual-ocular control is working properly. The last phase of ENG is a caloric test. The purpose of this phase is to simulate the vestibulo-ocular reflex. In this phase approximately 20ml cool water or air is injected into the subject's ear canal and stimulated eye movements are recorded. Cool water or air causes the liquid motion in the vestibular organ which in turn causes nystagmus. Nystagmus caused by cool water or air disappears within approximately five minutes. In some cases this test can reveal the side of malfunctioning vestibular organ.

The rotation test can also be done with a computer, but in its simplest form it only requires a rotating chair. In this case a physician rotates a subject on a rotating chair and makes a subjective evaluation about the state of the vestibulo-ocular reflex.

Computerized dynamic posturography [1, 46] can be used to test the function of the motor control system of a subject. In this test a subject stands on a force platform which is explained in Section 4. During CDP a subject can be exposed to different visual stimuli or other external disturbances. The force platform records the movements of a subject which can be analyzed after the test. Because the result of CDP contains all the corrective movements which are required to maintain the balance, it can be seen as a test which tells how well the different subsystems of the balance control work together. This also allows the possibility to block certain information channels. For instance, the effect of vision on balance controlling can be studied by blindfolding. Also, proprioceptive information from the ground can be suppressed by vibrators which are attached to both calves [82].

In the field of medical expertise the ability to make a correct diagnosis is important. In certain cases diagnosing is easy. For instance, flu can be easily verified with a thermometer and visual inspection. Unfortunately, there are diseases which are hard to diagnose certainly. Among them there are diseases which cause vertigo and balance disorders [10, 30 and 69].

The diagnosing of complicated diseases requires many different tests and an interpretation of the interconnections of their results. This can be exhaustive, error-prone and there might be subjective variation in the resulting diagnoses. To remove the burden of diagnosing procedure and to get more consistent results the use of an expert system could be reasonable.

An expert system [45, 81] is software which attempts to simulate the work of a human expert. Such a system contains a set of rules which operates on input data and relates it to certain outputs (here, diagnoses). The form of input data, rules and outputs of a system are thoroughly studied among the large group of experts. Experts have "taught" the system to respond correctly in the various input cases.

Another way to teach such a system is to use artificial intelligence or machine learning methods. The mapping of input data to output is searched with the computer. In this thesis the author used this approach. Of course, the origin and the nature of input data must be known beforehand.

After an expert system is built it has to be tested. During testing a set of test cases is input to the system. The results of the system are compared to the results of a set of human experts. If the results of an expert system are comparable to those of the human experts, it can be considered useful.

4 Data collection

4.1 Equipment

In postural control research the most common measurement device is a force platform [1, 11]. A basic version of a force platform resembles a circle shaped scale. It contains three force sensors which record vertical force reactions against the surface of the platform. The arrangement of the sensors forms a triangle in which the sensors form a plane. If we now consider that a constant dot shaped force **F** is acting downwards inside the triangle depicted in left side of figure 4.1, we can use the Newton's third law to get the relations of the forces

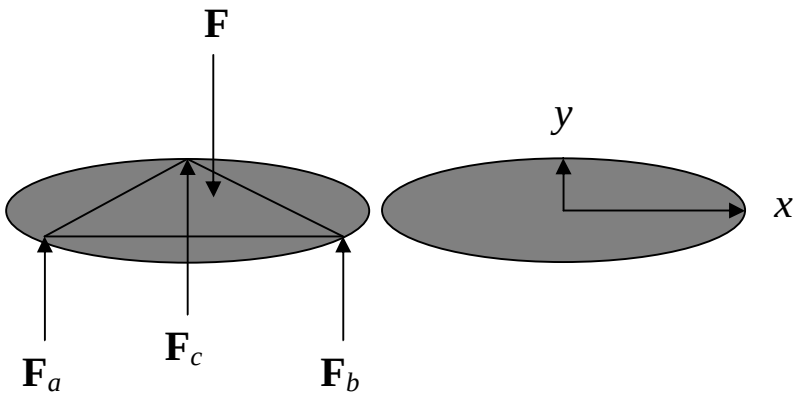

Figure 4.1: Illustration of force platform from the back and its *xy* plane.

$$\mathbf{F}=\mathbf{F}_a+\mathbf{F}_b+\mathbf{F}_c. \quad (4.1)$$

The locations of the forces $\mathbf{F}_a$, $\mathbf{F}_b$ and $\mathbf{F}_c$ are always the same and only the position of **F** can change on the *xy*-plane. If we fix the origin of the force platform to the centre of the circle such that the *x* axis points at the right and *y* axis points straight ahead, we can form the moment equations about the *x*- and *y* axes.

$$\mathbf{M}x=\mathbf{F}_a l+\mathbf{F}_b l+\mathbf{F}_c c+\mathbf{F}y=\mathbf{0}, \quad (4.2)$$

$$\mathbf{M}y=\mathbf{F}_a a+\mathbf{F}_b b+\mathbf{F}x=\mathbf{0}, \quad (4.3)$$

where l is the perpendicular distance of bisector ab from the origin, c is the y coordinate of $\mathbf{F}_c$ from the origin, a is the x coordinate of $\mathbf{F}_a$ from the origin and b is the x coordinate of $\mathbf{F}_b$ from the origin. The location of **F** is given by x and y. The force platform can be calibrated accurately if we use Newton's third law, gravitational acceleration g and accurate test mass m. The calibration is needed because the sensors measure only a voltage which changes due to an acting force **F**. The relation between the acting force **F** and the voltage readings from sensors U_a, U_b and U_c are considered to be linear when the **F** is caused by a mass of a normal weighted subject. The calibration coefficients for the sensors can be obtained by solving a linear equation

$$F=aU_a+bU_b+cU_c+e, \quad (4.4)$$

where F is the magnitude of $\mathbf{F}$, a, b and c are the calibration coefficients of the respective sensors and e contains the summed biases from all sensors. When the force platform is calibrated, we can calculate the mass of a subject and the location of the centre point of pressure (COP) under the feet by using the force and moment equations (4.1), (4.2) and (4.3).

In addition to the force platform balance measurements have also been done by using a camera [27, 83] and inertial based devices [9, 80]. They are usually planned and built balance measurements in mind. A part of the present thesis deals with balance measuring with a commercial magnetic tracking device. The motivation was that the tracking device is cheaper than a force platform and it provides more flexibility in the implementation of different balance test setups. For instance, the magnetic tracking device can be used to explore how a subject uses the arms to maintain balance. Also, head and hip movements can be captured.

The tracking device used was a Nest of Birds from Ascension Technology Corporation [37]. This device is usually employed in the virtual reality environments for capturing human motions, which are quite difficult and time consuming to model with mathematical methods. The tracking device consists of three main components presented in figure 4.2. On the right part of figure 4.2 there is the actual tracking device which can be connected to the computer with the universal serial port (USB). On the left the cube shaped object is a transmitter used to create a magnetic field. In the middle of the figure there are four sensors which are able to measure their position (x,y,z) and rotation (α,β,γ) about the respective axes in the created magnetic field. One of the sensors is attached to a headband and the other can be attached to the wrists, for instance.

Figure 4.2: Magnetic tracking device

The structure of a tilting force platform is similar to the basic version but, in addition, it provides a possibility to rotate its surface about the anterior-posterior (x) and medio-lateral (y) directions. We have to take account the inertial moment of the platform J and its angular accelerations α_x and α_y about the x and y axes. This gives the moment equations

$$\mathbf{M}_x=\mathbf{F}_a l+\mathbf{F}_b l+\mathbf{F}_c c+\mathbf{F}y=J\alpha_y \quad (4.4)$$

$$\mathbf{M}_y=\mathbf{F}_a a+\mathbf{F}_b b+\mathbf{F}x=J\alpha_x, \quad (4.5)$$

which make it possible to get the subject's mass m and the centre point of force (x,y) beneath the feet. The primary benefit from the use of the tilting force platform is that

it is possible to disturb the stance of a subject standing on it. This forces the subject to actively support on his or her postural control system. A tilting force platform is presented in figure 4.3.

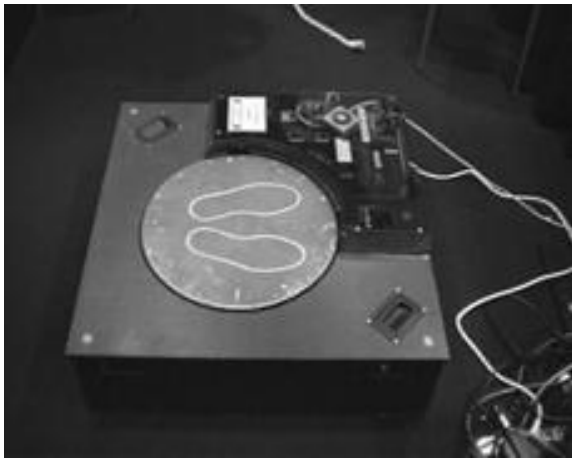

Figure 4.3: A tilting force platform

Another way to disturb a subject's balance is to provide him or her some visual information which is in contradiction with the environment where the subject actually resides [35, 77, 78, 79]. This is the case because humans support heavily on their vision when maintaining balance [8, 72]. An easy way to create such environments is the use of virtual reality. These environments are usually implemented with OpenGL [33, 70] or Direct3D [36, 55] and they are provided to a user through a head mounted display (HMD). An HMD has two displays, one for each eye. Virtual reality software creates two images from the environment which are quite similar. The only difference between these images is that there is about a 58mm gap [68] between their centre points of projections. This creates an illusion of a three dimensional environment and immerses a subject into it [17, 49, 62]. A V8 HMD applied from Virtual Research Systems [42] is presented in figure 4.4.

Figure 4.4: A head mounted display

The software, which connects all the devices mentioned above, collects measured data and makes it possible to show different virtual stimuli to a user, was planned and implemented by Tossavainen [76]. It is implemented in C and it includes such software libraries as Simple DirectMedia Layer (SDL) [40], OpenGL, driver library

for the magnetic tracking device, driver library for the orientation sensor on HMD [39] and driver library for DT 9800 analog digital (AD) converter [38].

4.2 Data

In the previous chapter the basic functions of two different force platforms were presented when a static dot shaped force is acting on them. In the postural control research the main goal for a computer scientist is to model the process when a subject stands on the force platform. A researcher has to decide how long a single test takes time. Usually the lengths of tests are between 15-60 seconds [16, 89]. The result of a single test is a three-dimensional time series whose length depends on the sampling frequency of an AD converter used to sample the force sensors of the force platform. The sampling frequency used was always 50Hz. A resulting time series is called a stabilogram and its components $[x_t,y_t,m_t]^T$ at every sampling instant t are the x and y components of COP and the mass m of a subject. Actually, the mass of a subject remains the same during a measurement and m can be considered as a force reaction caused by a subject's mass. To clarify a stabilogram an example in xy plane is given in figure 4.5. In figure 4.6 the same stabilogram is presented componentwise.

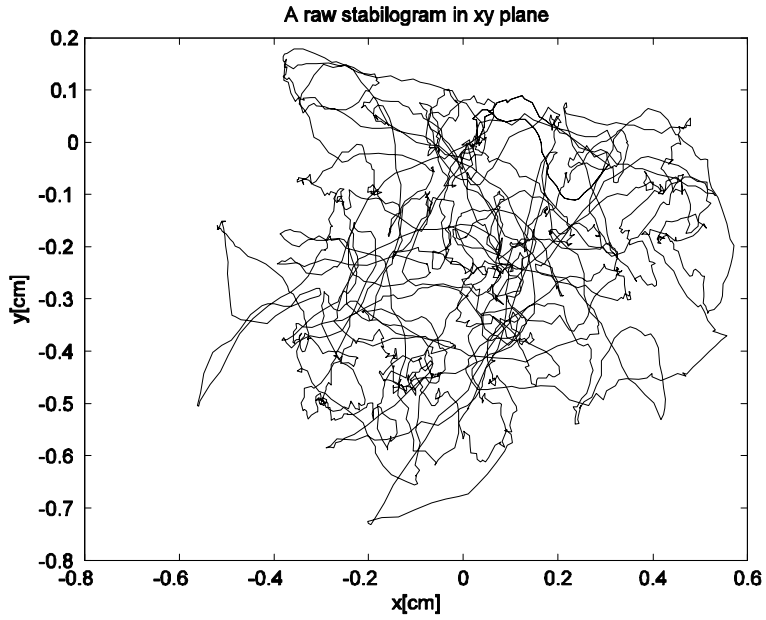

Figure 4.5: A raw stabilogram signal from a random subject

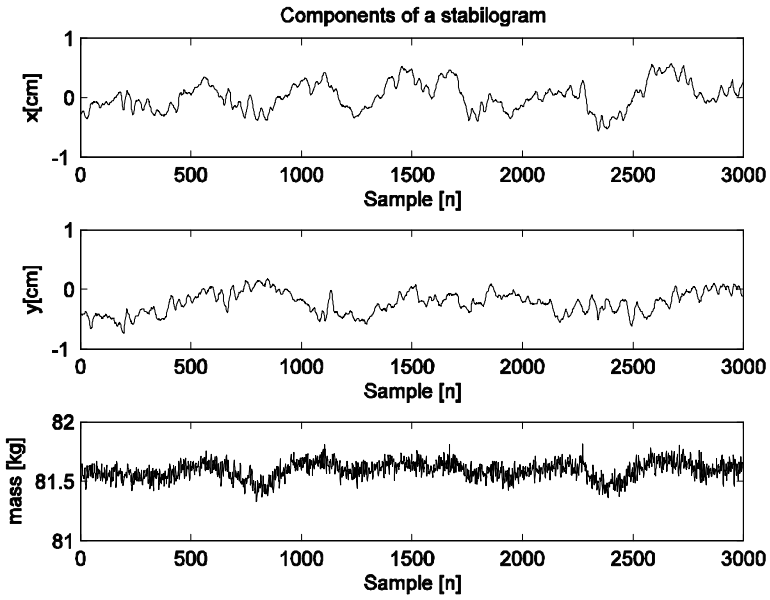

Figure 4.6: A stabilogram divided into its components

The Nest of Birds tracking device can measure the positions and orientations of the attachment points of its sensors. However, we used only the position information. We selected this approach because rotations during quiet stance were small and rotations also affect the position information. For instance, if a unit cube is rotated about its centre, the new locations of its vertices can be calculated by the magnitude and direction of the rotation angle. Data from the tracking device resembles that from the force platform. However, instead of the mass there is an additional *z* coordinate. In addition to this, the sampling frequency of the tracker is 33.3Hz which means that measured signals are shorter than force platform signals. An example signal from the tracker in *xy* plane is presented in figure 4.7 and the individual component signals are presented in figure 4.8. The example signal presents a subject's head movements.

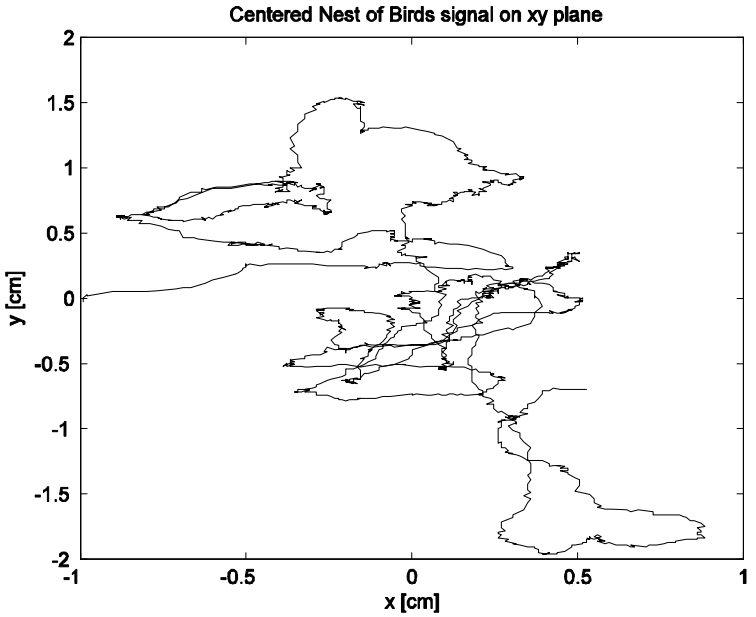

Figure 4.7: A centred raw Nest of Birds signal of a subject in *xy* plane

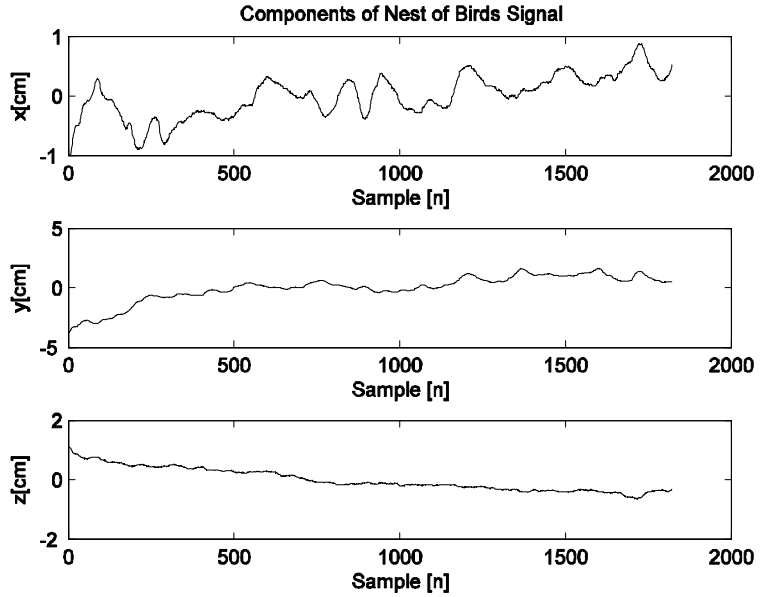

Figure 4.8: The components of a raw Nest of Birds signal of a subject

5 Features

When a data set is collected, the interesting information that characterizes an underlying problem is more or less buried in the data. It might be that the interesting information cannot be measured directly or the measurement is distorted due to environmental factors and inaccuracies in measurement devices. Depending on the quality of data, different levels of preprocessing might have to be applied. The most common preprocessing methods include the interference reduction with digital filtering in the case of time series data, and possible dimension reduction methods if the dimension of original data is large.

Despite the quality of the measured data, the set of procedures used to extract the essential part of information is called feature extraction and it results in a set of feature vectors. For instance, if we form a feature vector **D** which presents a dog it could have such components as weight *w* and height *h*. In this case $\mathbf{D}=[w\ h]^T$. On the other hand, there could be several other feature vectors that could also present a dog. A selection of feature vectors depends on their intended use. The selection of the best possible features can sometimes be very difficult and it might require computational methods [28, 75, 85]. However, usually a researcher has an insight for what would be useful features. In this case the useful features can be extracted from preprocessed data, for instance, with system identification methods [41, 53].

5.1 System Identification and linear digital filtering

As mentioned above, signals measured from real world processes contain interesting information and noise. Linear digital filtering [55, 61, 71] provides us a powerful tool to suppress a possible noise component in our measured signal if the noise resides in a different frequency band from the interesting part of a signal. If they are in the same frequency band, they cannot be separated by digital filtering. Figure 5.1 depicts a

situation where an input signal $x[t]$ goes through a digital system producing an output signal $y[t]$. The error term $e[t]$ acting on the system is usually unknown and it can originate from measurement devices, environment or too naive a mathematical model. As matter of fact, when we model a real system there is no such thing as a real model. However, it is possible to have several different models which are good enough approximations depending on a selected criterion.

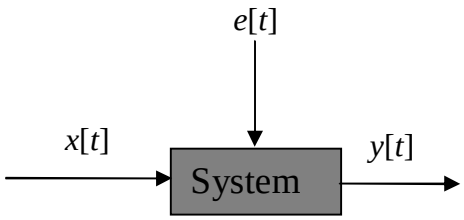

Figure 5.1: An illustration of a linear digital filter

The realisations of real world systems are dynamic in their nature. A system's output $y[t]$ is affected by its previous values $y[t\text{-}1],\ldots,y[t\text{-}m]$ and by the past input values $x[t],\ldots,x[t\text{-}n]$. We can give a difference equation which maps together these values as follows

$$y[t] = \sum_{i=0}^{N} b_i x[t-i] + \sum_{j=1}^{M} a_j y[t-j] + e[t]. \qquad (5.1)$$

Equation (5.1) describes an ARX-model [51]. This is only a possible model structure, but it is used in the field of both digital filtering and system identification. Usually, the error term $e[t]$ is considered to be independent of time, in other words, a stationary process. The assumption simplifies the process of system identification and. When the goal is to identify a system, then the task is to estimate the coefficients $[a_1, \ldots, a_m, b_0, \ldots, b_n]$ given the signals $x[n]$ and $y[n]$, which is typically done by linear regression [60] and using the least squares error criterion [60]. If an identified system is a noise process to be removed, we can estimate an inverse system. This can be done by inverting the roles of $x[n]$ and $y[n]$ in the (5.1) or to use the z transform [58] of (5.1) and to switch the roles of the numerator and denominator polynomials. In both cases, once a system is identified, its inverse system can be obtained from the coefficients $[a_1, \ldots, a_m, b_0, \ldots, b_n]$. When we invert the roles of $x[n]$ and $y[n]$ and leave out the error term $e[t]$, we get another difference equation which is

$$x[n] = \frac{1}{b_0}\left(y[n] - \sum_{j=1}^{M} a_j y[n-j] - \sum_{i=1}^{N} b_i x[n-i] \right). \qquad (5.2)$$

When we take the z transform of (5.1) we get

$$Y(z) = \sum_{i=0}^{N} b_i X(z) z^{-i} + \sum_{j=1}^{M} a_j Y(z) z^{-j}$$

$$Y(z)\left(1 - \sum_{j=1}^{M} a_j z^{-j} \right) = X(z) \sum_{i=0}^{N} b_i z^{-i}$$

$$H(z) = \frac{Y(z)}{X(z)} = \frac{\sum_{i=0}^{N} b_i z^{-i}}{1 - \sum_{j=1}^{M} a_j z^{-j}}.$$

If we multiply both sides of (5.2) by b_0 and take the z transforms from its both sides, we get

$$b_0 X(z) = Y(z) - \sum_{j=1}^{M} a_j Y(z) z^{-j} - \sum_{i=1}^{N} b_i X(z) z^{-i}$$

$$b_0 X(z) + \sum_{i=1}^{N} b_i X(z) z^{-i} = Y(z) - \sum_{j=1}^{M} a_j Y(z) z^{-j}$$

$$X(z)\left(b_0 + \sum_{i=1}^{N} b_i z^{-i} \right) = Y(z)\left(1 - \sum_{j=1}^{M} a_j z^{-j} \right)$$

$$\overline{H}(z) = \frac{X(z)}{Y(z)} = \frac{1 - \sum_{j=1}^{M} a_j z^{-j}}{\sum_{i=0}^{N} b_i z^{-i}}$$

If we now look at $H(z)$ and $\overline{H}(z)$, we notice that they are inverses of each other. Once a noise system is identified, its inverse system can be used to suppress noise. The concepts of linear digital filtering and system identification are closely related. In system identification we estimate the coefficients [a_1, …, a_m, b_0, …, b_n] which can be considered as a feature vector of an identified system. In linear digital filtering we actually use the identified system to enhance our measured signals.

5.2 Dimension reduction

In an ideal case a single feature vector contains only such components that are necessary for an intended application. However, many times a feature vector contains more components than is necessary from applications point of view. In this case we have to remove such components from original feature vectors which contain redundant information. Sometimes it is possible to remove individual components, but usually we have to form new features which are different combinations of original feature vector components. Regardless of an application all individual feature vectors are usually collected together into an observation matrix. In an observation matrix the number of rows is equal to the number of feature vectors and the number of columns is equal to the dimension of feature vectors. If the dimension is high, it can cause serious computational burden. Especially, when the computational complexity [2] of an algorithm used is high. For instance, if the computational complexity of an algorithm is of $O(d^2)$ where d is the length of a feature vector, it would be useful to find a presentation to the original feature vectors which contain almost all information in a shorter form $d' << d$.

Probably the most common way to reduce the dimension of original feature vectors is the principal component analysis (PCA) [43, 47]. The basic idea in PCA is to reduce the dimension of feature vectors in a way that we lose as little of the variance of original feature vectors as possible. The first step is to find such a linear combination of feature vector **x** that has the greatest possible variance. The variance of such linear combination is

$$\mathrm{Var}(\mathbf{q}^T\mathbf{x})=\mathbf{q}^T\mathbf{\Sigma}\mathbf{q}, \tag{5.3}$$

where **q** is a vector of coefficients of a linear combination and **Σ** is the covariance matrix of all feature vectors. Now our task is to find out such **q** that maximizes

$$\mathbf{q}^T\mathbf{\Sigma}\mathbf{q}, \tag{5.4}$$

with the constraint that

$$\mathbf{q}^T\mathbf{q}=1. \tag{5.5}$$

Without the constraint the maximum would not exist. This gives us an equation

$$f(\mathbf{q})=\mathbf{q}^T\mathbf{\Sigma}\mathbf{q}-\lambda\mathbf{q}^T\mathbf{q}. \tag{5.6}$$

The maximum of (5.6) can be obtained by taking the derivative with respect to **q** and equate the result to zero. This gives us

$$\left(\frac{\partial(\mathbf{q}^T\Sigma\mathbf{q}-\lambda\mathbf{q}^T\mathbf{q}}{\partial\mathbf{q}}\right)=(\Sigma+\Sigma^T)\mathbf{q}-\lambda(\mathbf{I}+\mathbf{I}^T)\mathbf{q}=\mathbf{0}. \tag{5.7}$$

Identity matrix **I** and covariance matrix **Σ** are symmetric, so (5.7) can be written in form

$$\Sigma\mathbf{q}=\lambda\mathbf{q}. \tag{5.8}$$

This formula is well known from linear algebra and it says that the vector **q** which maximizes (5.6) is the eigenvector of **Σ** and λ is its respective eigenvalue. According to [47] λ is the greatest eigenvalue of **Σ** and **q** is the normalized respective eigenvector. The variance of original feature vectors is greatest in the direction of **q**. If we search for the direction **v** which yields the direction of the next greatest variance among feature vectors the procedure is the same as above, but we have to add a constraint that $\mathbf{q}^T\mathbf{x}$ and $\mathbf{v}^T\mathbf{x}$ are uncorrelated. We obtain

$$\mathrm{Cov}(\mathbf{q}^T\mathbf{x},\mathbf{v}^T\mathbf{x})=\mathbf{q}^T\mathrm{Cov}(\mathbf{x},\mathbf{x})\mathbf{v}^T=\mathbf{q}^T\mathbf{\Sigma}\mathbf{v}^T=0. \tag{5.9}$$

When we continue this process, we finally end up to a situation where all possible linear combinations are found which maximizes the variances of the original feature vectors in their respective directions. According to [47] it turns out that these linear combination vectors are the eigenvectors of **Σ** in such an order that the direction of the first eigenvector yields the greatest variance and the last one gives the smallest variance.

Almost all real world measurements contain errors and disturbance which cannot be accurately explained. From this viewpoint we can consider that the small variance that is accounted in the directions of a few least variance eigenvectors can be left out of further inspection as noise. Now we can present a vector $\mathbf{x}=[x_1, x_2,\ldots,x_{d-1}, x_d]^T$ in the form of $\mathbf{p}=[p_1,p_2,\ldots p_{d'-1},p_{d'}]^T$ where $d'<d$ and the relation between **x** and **p** can be

written in form **p**=**Ax**. The matrix **A** contains the eigenvectors of the original covariance matrix from the first to the mth as its rows as follows

$$\mathbf{A} = \begin{bmatrix} q_{11} & . & . & q_{1n} \\ q_{21} & . & . & q_{2n} \\ . & . & . & . \\ q_{m1} & . & . & q_{mn} \end{bmatrix}. \qquad (5.10)$$

The selection of the number of principal components depends on an intended application. A common practice is to select so many principal components as needed to capture 80% of the original variance of a feature vector set.

6 Machine learning and methods applied

A healthy person is constantly making observations from the surrounding world. He or she can recognize a friend on the basis of the voice or the way this is walking. Also, the recognition of different materials is easy on the basis of their texture, odor or some other characteristics. The recognition is possible due to senses and learning. For instance, a little child might not have an idea what berries are poisonous and what berries are not. However, under the guidance of an adult a child gradually learns to separate these situations.

A result from the recognition stage suggests us to take an action. For instance, if we hear a friend's voice from a crowd, we try to locate the friend. An unknown voice does not necessary lead to any action. In other words, we perform classification on the basis of recognized or unrecognized events.

The learning mechanism of computers tries to imitate the human learning mechanism. The main difference is that computers can only deal with numbers. A user of a computer should convert real world phenomena into a set of feature vectors discussed in Section 5. For instance, a human voice can be depicted with a vector which contains the most dominating frequency components of a sample voice.

Machine learning can roughly be divided into two distinct phases, learning and classification. Despite the actual structure of a machine learning method the first phase is to teach the system. A teacher labels the test samples and presents these to the system. At the same time the teacher tells the system into which group the particular sample belongs to. This method is called supervised learning [19]. Another learning scheme is so called unsupervised learning [19], where there is no teacher intervention. In this case the learning process tries to cluster the data into separate classes. This learning method is usually used in the preprocessing stage. If data forms separate classes according to some feature vector component, this component is important and should be included in the final feature vector.

Another phase in machine learning is to use a trained system for prediction purposes. We input such a feature vector to the system that has not been "seen" before. On the basis of its internal logic the system "scores" the sample feature and this "score" determines the location in the feature vector space. In short, we try to predict the class to which an unknown feature vector belongs. A very intuitive way to describe the prediction is the use of classifier functions [19]. A trained system may contain a set of classifier functions $g_1(\mathbf{x}),\ldots,g_c(\mathbf{x})$, where c is the number of possible classes. In the

training phase the boundaries between the classes have been fixed and these are called decision boundaries [19]. For the prediction we calculate the values of $g_i(\mathbf{x})$ for all i and make a decision that $\mathbf{x}$ belongs to class i if $g_i(\mathbf{x})>g_j(\mathbf{x})$ for all $i\neq j$. In the next six subsections the machine learning and filtering methods used in this thesis are presented.

6.1 Hidden Markov models

The conventional time series analysis proposes that the signals under the study are stationary in the weak sense. Then the mean and variance of a time series do not depend on time. The dependence of successive time series values can be captured by the autocorrelation structure of the process which generates the time series in question. The family of hidden Markov models [11, 13, 63] adds more flexibility to the structure of time series by adding a possibility to jump between signal sequences with different means and variances. In addition, the "hidden" structure makes successive time series values conditionally independent. This simplifies the modelling of the dependence between time series values. In this thesis we consider only such hidden Markov models that can have continuous observation values. Discrete models are considered in [63].

A hidden Markov model (HMM) is a stochastic automaton which consists of a set of hidden states $Q=\{Q_1,\ldots,Q_n\}$, probability vector $\boldsymbol{\pi}$ which contains the probabilities for the starting state where the automaton begins, a transition matrix $\mathbf{A}$ which gives the transition probabilities between hidden states, and a matrix $\mathbf{B}$ which contains the probability density functions associated to hidden states. A common way to depict a hidden Markov model is the use of triplet $\lambda=(\boldsymbol{\pi},\mathbf{A},\mathbf{B})$. A three state hidden Markov model is presented in figure 6.1. The components of matrix $\mathbf{A}$ are marked as a_{ij} and the components of matrix $\mathbf{B}$ are marked as $f_i(\mathbf{x})$.

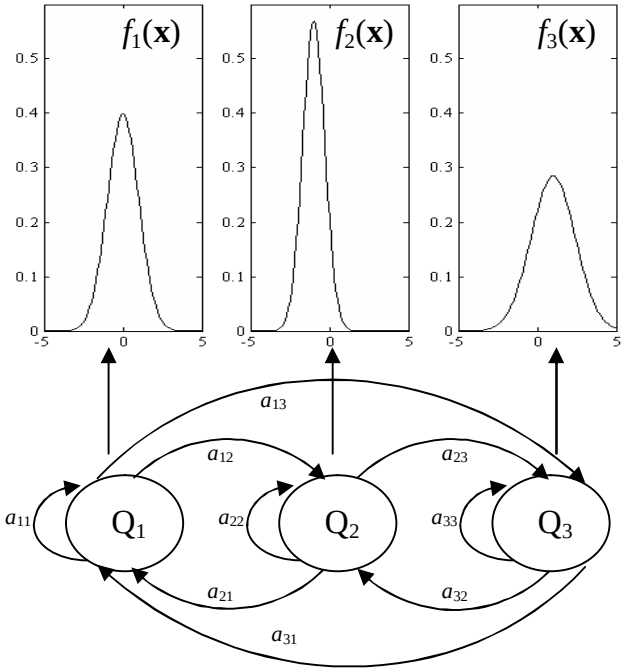

Figure 6.1: An illustration of a hidden Markov model

The use of hidden Markov models usually contains two stages which are the training and classification. In the training stage we find the parameters $\boldsymbol{\pi}$, **A** and **B** which give the highest logarithmic likelihood for the training data. A logarithmic likelihood function is used because it is easier to evaluate than the original likelihood function. The most common training algorithm is the Baum-Welch algorithm [63].

In the classification stage we have n trained hidden Markov models $\{\lambda_1,\ldots,\lambda_n\}$ which are trained with signals from n different signal sources. An unknown signal is presented to all n models and it is classified into the class whose model gives it the highest logarithmic likelihood. The likelihood of an unknown signal $O=\{O_1,..,O_T\}$ along one possible path is calculated as follows:

1. Select the starting state i according to $\boldsymbol{\pi}$.
2. Calculate the probability density function value for observation O_1 in state i according to **B**.
3. Make a transition from state i to the state j according to **A**.
4. Continue from stage 2 until the observation O_T is reached

The final likelihood is obtained by summing over all possible paths through the model. The calculation of the final likelihood of an observation signal with a brute force method is prohibitive because the number of possible state permutations is large. An efficient algorithm exists and it is depicted in [63].

6.2 Discrete Kalman filters

Kalman filters are a family of recursive filters which operate on a pair of stochastic equations. This equation pair is usually called a state space model [53, 20] and it can be given in a form

$$\mathbf{r}_t=\mathbf{A}\mathbf{r}_{t-1}+\mathbf{w}_{t-1}, \tag{6.1}$$

$$\mathbf{z}_t=\mathbf{H}\mathbf{r}_t+\mathbf{v}_t. \tag{6.2}$$

The first equation models the dynamics of a system under study. Vector $\mathbf{r}_t$ is the internal state of a system at time instant t (for instance the components of **r** could be position, velocity and acceleration). This state is hidden from the user and the purpose of a Kalman filter is to estimate this state. A transition matrix **A** relates the previous state $\mathbf{r}_{t-1}$ and the current state $\mathbf{r}_t$ together and $\mathbf{w}_{t-1}$ is the noise component in the dynamic model at time instant $t-1$. The successive **w** realizations are considered to be uncorrelated and their distribution is considered to be an d dimensional normal distribution $N(\mathbf{0},\mathbf{Q})$, where **Q** is the covariance of a model noise process.

The second equation is a measurement equation and it relates the systems internal state $\mathbf{r}_t$ and measured or observed state $\mathbf{z}_t$ through the observation matrix **H**. Vector $\mathbf{v}_t$ is a measurement error at time t. The measurement errors are considered uncorrelated and their distribution is an d' ($<d$) dimensional normal distribution $N(\mathbf{0},\mathbf{R})$, where **R** is the covariance of measurement errors. The model noise **w** and the measurement noise **v** are also considered uncorrelated.

Because the correct system state $\mathbf{r}_t$ is unknown, we have to predict it with equations (6.1) and (6.2). This gives us an a priori estimate $\mathbf{s}_t=\mathbf{A}\mathbf{s}_{t-1}$. In this case the previous

state is also an estimate. A common way to initialize a Kalman filter is to set the initial state $\mathbf{s}_0$ to a null vector [53, 86]. After a prediction we can take an actual measurement $\mathbf{z}_t$ from the system. The measurement $\mathbf{z}_t$ can be used to correct the prediction $\mathbf{s}_t$ and we get the a posteriori estimate of $\mathbf{s}_t$. This can be given in the form

$$\mathbf{p}_t=\mathbf{s}_t+\mathbf{K}(\mathbf{z}_t-\mathbf{H}\mathbf{s}_t), \tag{6.3}$$

which is a linear combination of the a priori estimate of $\mathbf{r}_t$ and the measured process state $\mathbf{z}_t$. In formula (6.3) $\mathbf{H}\mathbf{s}_t$ is an estimate of $\mathbf{z}_t$ and the $\mathbf{K}$ is a Kalman gain [53, 86] which weights the measured values $\mathbf{z}_t$ and its predicted version $\mathbf{H}\mathbf{s}_t$. If the covariance of measurement noise $\mathbf{R}$ approaches zero, the Kalman gain approaches $\mathbf{H}^{-1}$ [86] and the a posteriori estimate $\mathbf{s}_t$ of $\mathbf{r}_t$ is not reliable at all. Thus the model only "trusts" the measured value $\mathbf{z}_t$. If the covariance of process noise $\mathbf{Q}$ approaches zero, the model does not "trust" the measurement $\mathbf{z}_t$ but only the a priori estimate $\mathbf{H}\mathbf{s}_t$. Against to this background, the Kalman filter weights the measured and predicted values in the proportions of their uncertainty.

6.3 Neural networks

The theory and applications of linear models are well understood and they are applicable to many real world problems. However, in some cases the ability of models to capture nonlinearities in the data under the study is required. Therefore, the use of an artificial neural network (ANN) [7, 31, 54, 67] can be a good choice. A simple neural network can also be used as a linear model as in this thesis. The motivation for the use of a neural network was primarily the comparison of different simple methods for the assessment of a feature vector describing the human swaying process. Like its name suggests, the structure of an artificial neural network is based on the simplification of human neural system. This system consists of neurons which are connected with synapses. The neurons can be considered as data processing units including some function f whose purpose is to process the input data in a predefined manner. The role of synapses is to weight the input data with weights $\mathbf{w}$ and to work as input data medium.

All the information a person can get from the environment is handled by one of the five senses, i.e. different neurons are sensitive to different impulses from the surrounding world. For instance, the use of vision activates the visual cortex in the rear part of the brain. Similarly the taste, smell, hearing and sense of feeling activate the different areas in the brain. This concept is used in artificial neural networks. In practice, a certain type of input data (information from the environment) is mapped to a certain area in an output vector space (brain). Depending on the area on which the input data is mapped different actions can be made. A simple two-layer neural network is presented in the left side of figure 6.2. The input for this network is a two dimensional vector (x,y) and the output tells whether the given input vector belongs to the shaded square in the right side of figure 6.2. In figure 6.2 dist($\mathbf{w}_i$) is the distance of an axis aligned straight line from origin which is perpendicular to direction $\mathbf{w}_i$.

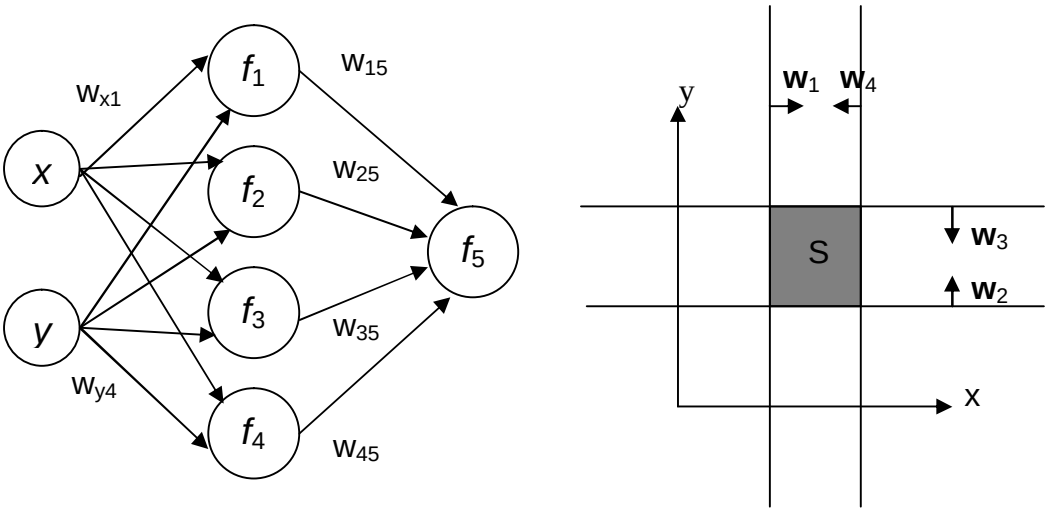

Figure 6.2: A two layer neural network and its intended decision boundary S

The internal working of the example neural network goes as follows:

1. A vector (x,y) is input to the network.
2. In all neurons 1,…,4 dot products added with the distance of limiting planes from origin are calculated $(x,y)\bullet\mathbf{w}_1+\text{dist}(\mathbf{w}_1)+,\ldots,+(x,y)\bullet\mathbf{w}_4+\text{dist}(\mathbf{w}_4)$ and their signs are recorded in functions $f_1,\ldots,f_4$.
3. The output is the sum of the outputs from functions $f_1,\ldots,f_4$.
4. If the sum is 4, the given vector is in the shaded region S. In any other case the given vector (x,y) is outside the region S.

For instance, if $\mathbf{w}_1=(1,0,1)^T$, $\mathbf{w}_2=(0,1,1)^T$, $\mathbf{w}_3=(0,-1,2)^T$ and $\mathbf{w}_4=(-1,0,2)^T$ where the two first components of $\mathbf{w}_i$ gives the direction of the perpendicular half spaces which are around the shaded area S and the third component of $\mathbf{w}_i$ gives the distance of each individual axis aligned straight line from origin. If we now test whether the tip of vector $(1.5,1.5)^T$ is inside the S we get $(1.5,1.5)\bullet(1,0)+1+(1.5,1.5)\bullet(0,1)+1+(1.5,1.5)\bullet(0,-1)+2+(1.5,1.5)\bullet(-1,0)+2$. Now for each $(x,y)\bullet\mathbf{w}_i+\text{dist}(\mathbf{w}_i)>0$ and this means that all f_i gets the value of 1 and $f_1+f_2+f_3+f_4=4$. As a result the tip of a vector $(1.5, 1.5)^T$ is in the shaded region S.

In the previous example the weights **w** and functions *f* were given because the simple problem was well defined. In real neural network applications the output regions are usually not known and they have to be calculated from the data. One of the most familiar ways to find the mapping between the input data and output regions is to use the backpropagation algorithm [7, 31, 54, 67]. This algorithm efficiently calculates the weights **w** when the forms of functions f_i are given. In practise, this is the teaching process of the network and it needs a "teacher" who tells the network which training sample belongs to which class.

6.4 Fisher's linear discriminant

In most classification problems the sets of feature vectors from different classes overlap a lot. However, if we can find a direction **w** from the feature vector space which separates cases between different classes, the classification becomes easy. In

this case we can use a dot product which projects the feature vector **x** on the line of a direction **w**. The location of the projection of **x** on **w** is a single scalar

$$y=\mathbf{w}^T\mathbf{x}, \tag{6.4}$$

where T is the transpose operator. A simplified example in the two-dimensional feature vector space is given in figures 6.3 and 6.4. In figure 6.3 two feature vector sets are presented, c_1 with dots and c_2 with plus marks. Their respective means $\mathbf{m}_1$ and $\mathbf{m}_2$ are projected onto a line which goes in direction **w**. From this figure we can see that the selection of **w** is not successful. If we project the remaining points from both classes onto line **w**, the projections will merge and we cannot make any classification.

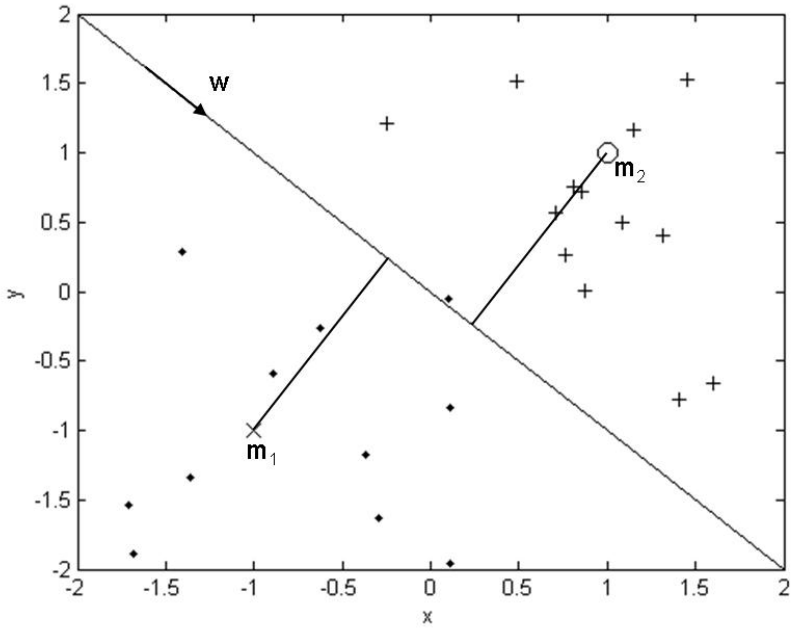

Figure 6.3: A direction w cannot separate the projections of two feature classes with means $\mathbf{m}_1$ and $\mathbf{m}_2$

In figure 6.4 an improved situation is presented. Vector **w** is calculated with the formula

$$\mathbf{w}=\mathbf{S}^{-1}(\mathbf{m}_2-\mathbf{m}_1) \tag{6.5}$$

where **S** is the covariance matrix of whole data set. The derivation of the formula is given in [19]. From figure 6.4 we can see that all samples from both groups can be classified correctly by projecting them onto the line **w** in the same manner as the means $\mathbf{m}_1$ and $\mathbf{m}_2$ are projected. In this case the values of equation (6.4) are clearly different for feature vectors from class c_1 and c_2.

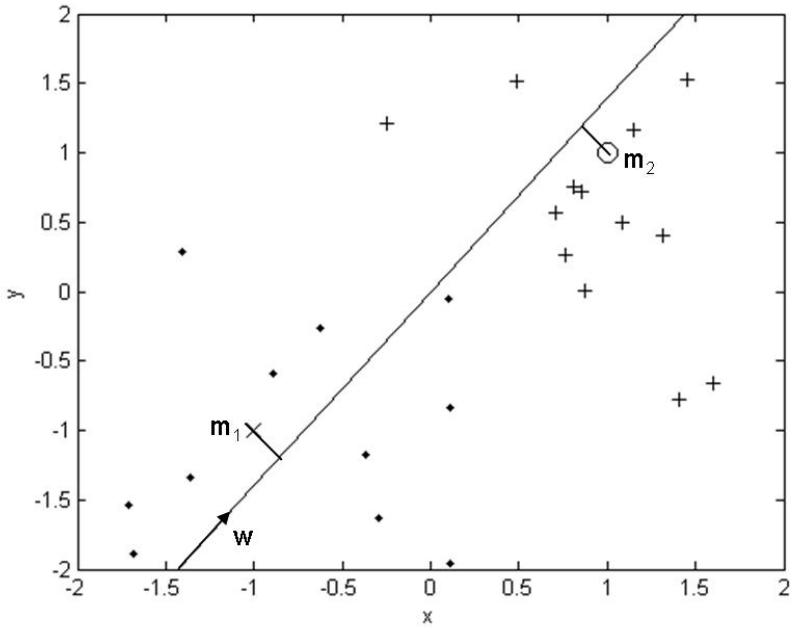

Figure 6.4: Vector w is the Fisher's linear discriminant which efficiently separates the projections of the two classes with means $\mathbf{m}_1$ and $\mathbf{m}_2$

6.5 *k*-nearest neighbour

The idea behind the classification with the *k*-nearest neighbour algorithm (kNN) [19] is intuitive. In its simplest form we have only three feature vectors $\mathbf{x}_1$, $\mathbf{x}_2$ and $\mathbf{z}$. The classes of feature vectors $\mathbf{x}_1$ and $\mathbf{x}_2$ are known and they are c_1 and c_2. The class of feature vector $\mathbf{z}$ is unknown and our task is to classify it on the basis of $\mathbf{x}_1$ and $\mathbf{x}_2$. Now we have to decide which of the feature vectors $\mathbf{x}_1$ and $\mathbf{x}_2$ is more "similar" with $\mathbf{z}$. If $\mathbf{z}$ "resembles" more $\mathbf{x}_1$ than $\mathbf{x}_2$, it is classified into the class c_1 and otherwise into c_2.

When working with real data sets the situation is usually more complex than above. The data vectors from different classes overlap and the classification based on only one nearest neighbour is more uncertain. To reduce uncertainty we can increase the number of nearest neighbour *k*. We seek for *k* nearest neighbours and we classify an unknown feature vector $\mathbf{z}$ to the class *c* which contains the majority of "similar" feature vectors. Figure 6.5 clarifies this aspect. In figure 6.5 an unknown feature vector $\mathbf{z}$ is marked with asterisk, three feature vectors belonging to class c_1 are marked with x:s and three feature vectors belonging to class c_2 are marked with circles. If we seek only one nearest neighbor, an unknown feature vector $\mathbf{z}$ is classified into class c_2 because the distance d_{1o} between $\mathbf{z}$ and a feature vector from class c_2 is the smallest. However, if we let the number of nearest neighbors to be three, a feature vector $\mathbf{z}$ is classified into class c_1 because one of three nearest neighbors belongs to class c_2 and two of them belong to class c_1.

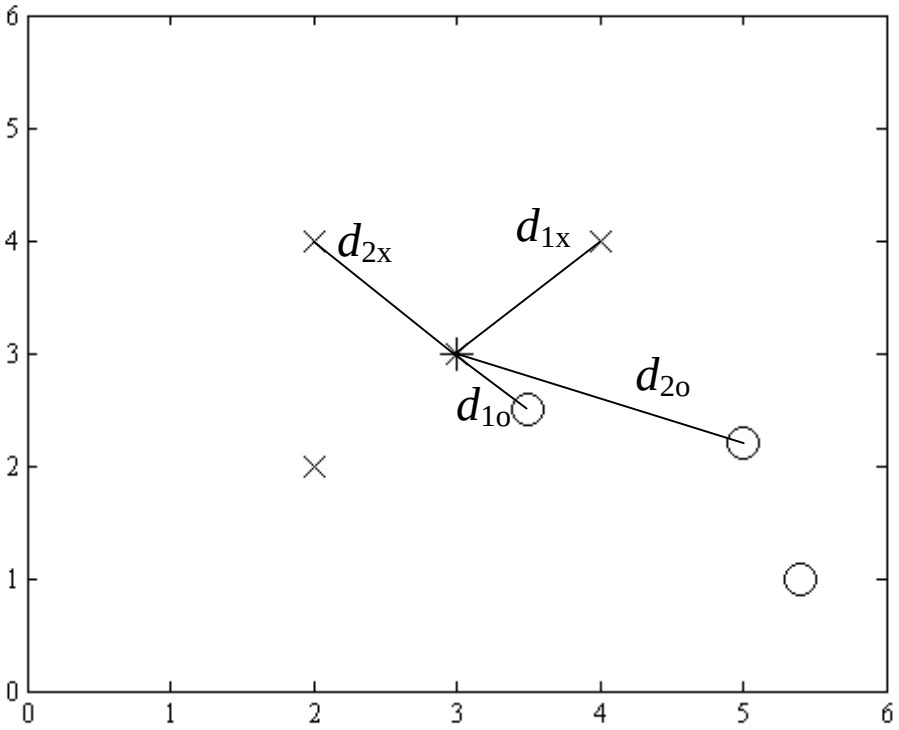

Figure 6.5: Idea of *k*-NN classification

The concept of similarity is usually given as a distance measure between feature vectors **x**, **y** and **z** which is ultimately context dependent. Depending on the application and the nature of feature vectors different metrics [73] can be used as a measure of similarity. A metric *d* has the following properties.

$$d(\mathbf{x},\mathbf{y}) \geq 0$$

$$d(\mathbf{x},\mathbf{y}) = 0 \text{ if and only if } \mathbf{x} = \mathbf{y}$$

$$d(\mathbf{x},\mathbf{y}) = d(\mathbf{y},\mathbf{x})$$

$$d(\mathbf{x},\mathbf{z}) \leq d(\mathbf{x},\mathbf{y}) + d(\mathbf{y},\mathbf{z})$$

The most common metric is the Euclidean distance between two vectors in a space. The Euclidean metric is also used in one part of this thesis (publication 4).

6.6 Mahalanobis distance

Mahalanobis distance [19] is a metric which takes account the way in which different components of feature vectors in a whole data set vary together. In figure 6.6 a random sample from two-dimensional normal distribution $\mathbf{x} \sim N(\mathbf{m}, \mathbf{\Sigma})$ is presented. In this case

$$\mathbf{m} = \begin{bmatrix} 2 \\ 2 \end{bmatrix} \tag{6.6}$$

$$\mathbf{\Sigma} = \begin{bmatrix} 1.0 & 0.7 \\ 0.7 & 1.0 \end{bmatrix}. \tag{6.7}$$

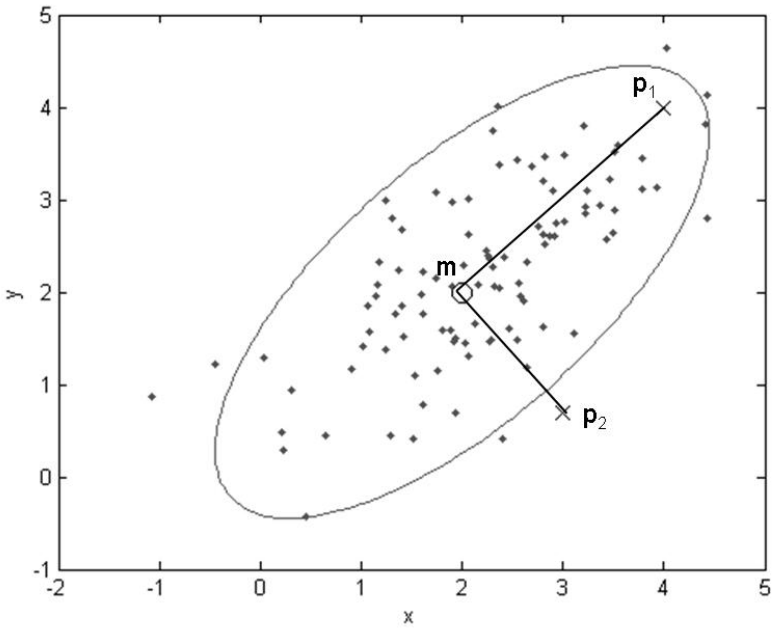

Figure 6.6: An illustration of Mahalanobis distance

Also, the 95 % confidence ellipse is drawn around all sample vectors. Here 95% of all sample vectors reside inside the confidence ellipse. In addition, the mean point **m** is marked with tiny circle; vectors $\mathbf{p}_1=[4\ 4]^T$ and $\mathbf{p}_2=[3.0\ 0.7]^T$ are marked with *x*'s.

The Euclidean distances from **m** to $\mathbf{p}_1$ and $\mathbf{p}_2$ are 2.8 and 1.6. However, the respective Mahalanobis distances are 2.1 and 2.2. For Mahalanobis distance point $\mathbf{p}_1$ is closer to **m** than point $\mathbf{p}_2$.

As we can see from figure 6.6 the *x* and *y* components of sample points **x** have strong linear dependence. As *x* grows *y* grows as well. This dependence is captured in the covariance matrix **Σ**. The covariance matrix **Σ** basically tells us the rotation and scaling of the original *x* and *y* axes. If we now wanted to express a feature vector **x** in the frame of the axes of the confidence ellipse, we should align these axes with the axes of original *xy*-coordinate frame. This is an inverse operation for the rotation and scaling of the confidence ellipse axes. Also, the origin of confidence ellipse should be translated to the origin of the *xy*-coordinate frame. Vector **x** in the frame of the confidence ellipse is

$$\mathbf{y} = \mathbf{\Sigma}^{-1}(\mathbf{x}-\mathbf{m}). \tag{6.8}$$

Now the Mahalanobis distance from **m** to **p** can be considered as a projection of scaled and rotated (**p**-**m**) on (**p**-**m**). Figure 6.7 presents a situation where points on the circle with radius 2 are multiplied with inverse of the covariance matrix **Σ**. The

Mahalanobis distances are calculated for all transformed points. The unit of the *x*-axis is given in degrees.

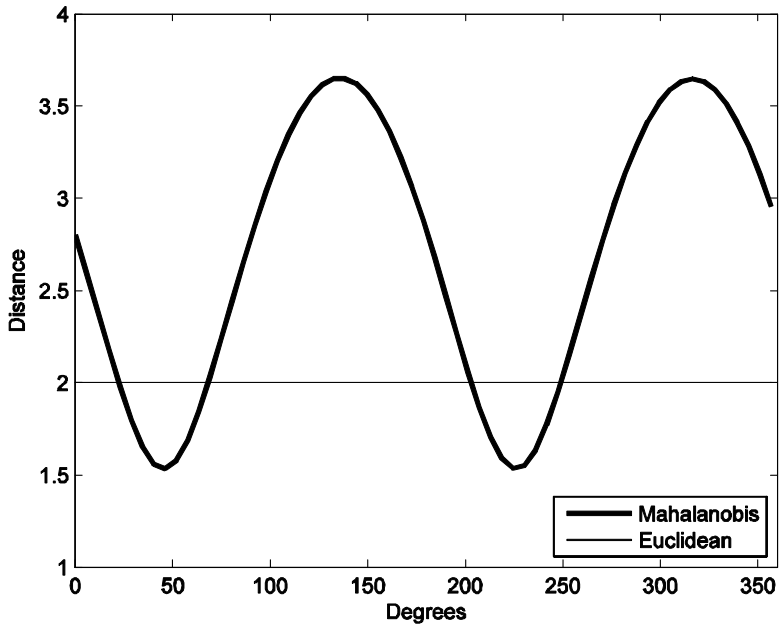

Figure 6.7: Mahalanobis distances of circle with radius 2 from origin

From figure 6.7 we can see that the points in the direction of longer main axis of the frame of the confidence ellipse are closer to the origin than the others in Mahalanobis sense. In figure 6.6 the direction of the longer main axis of the confidence ellipse is 45 degrees from the *x* axis.

7 Performance of a classifier

The assessment of the performance of a trained classifier must be done before using it. In an ideal case the recognition accuracy of a classifier can be tested with a large amount of data. Unfortunately, this is seldom possible. The collection of the real world data sets can be expensive, laborious or even dangerous leading to a situation where researchers have to deal with a limited amount of data.

The most desired characteristic of a trained classifier is its ability to accurately predict the class of an unknown feature vector. In order to achieve this ability two different validation schemes are required. First, the structure of a classifier should be studied and second, the performance of a classifier should be assessed. Depending on the application the structure of a classifier could be for instance, the value of k in k nearest neighbor classifier or the number of hidden nodes in a neural network.

Usually we want to fit a model such that its prediction error is as small as possible. For instance in linear regression we seek such parameters for the model which yields the minimum of the summed squared residuals. In general, this approach can cause a serious overfitting. The samples from data used in fitting procedure are predicted correctly but the prediction of an unknown data is uncertain. This phenomenon originates from the fact that the model has learned some degrees of noise which is present in the training of fitting data.

To avoid overfitting the original dataset is divided into two or three disjoint sets depending on the application. The use of these disjoint sets is called crossvalidation [7, 31, 54, 67]. The easiest dataset division is called a hold-out method. In this scheme the data is divided into two disjoint sets. One set is used in the training of a classifier and the other is used for evaluation of the classification error. The determination of a model structure can be done on the basis of the classification error. For instance the value of *k* in *k* nearest neighbor classification can be selected such that is yields the minimum classification error among all *k* values used as testing. After the decision of the model structure the hold-out method can be used in determining the performance of a trained classifier.

The hold-out method has certain drawback. It uses only one test and training set. If the split into training and test sets is unfortunate the estimate of the performance of a classifier is wrong. An approach for reducing uncertainty in the performance of a classifier is to use more separate training and testing sets. This is called cross validation. In this approach the whole dataset can be divided into *k* disjoint sets by using either predefined division or random permutation. Both of these methods are similar but the predefined division ensures that all data samples are used for training and testing. In random permutation this is not certain.

Despite the division method used the training and testing phase is repeated such that the classifier is trained by using *k-1* sets and tested with one set. In every repetition the error rate of the classifier is recorded. The repetition of training and testing is terminated when all *k* sets are used as a test set. The error rate of a classifier is the arithmetic mean of error rates of all individual test sets.

The selection of *k* depends highly on the available dataset. If there are plenty of data, the choice of the value of *k* is flexible, but in the case of a small dataset we may be forced to let the *k* to be equal to the size of the dataset. This method is called leave one out cross validation and as the name suggests, it leaves only one test case and uses all other in the training process.

Three-way split of a dataset is primarily used in training of a multilayer neural-network. In the three-way split one portion of the data is used for training, another part is used for testing the performance of a classifier and the third set, called the validation set, is used for terminating the training process. In this case the role of the validation set is to prevent the overfitting to occur. The training of a multilayer neural network is terminated when its generalization ability is about to reduce. In this point the classification error of the training set is diminishing but the classification error of the validation set starts to increase.

8 Results

The main research problem in this thesis was to explore whether it is possible to predict the state of a subject on the basis of the measured stabilogram and magnetic tracking device signals. The signals are measured using the force platform (publications 1, 2, 4 and 5) and the magnetic tracking device (publication 3). The state of a subject depends on the applied test setup.

In the first publication there were four different states. (1) A young healthy subject was standing on the force platform with the eyes open. (2) A young healthy subject was standing on the force platform with the eyes closed. (3) A person standing on the

force platform was young and healthy. (4) A person standing on the force platform suffered from Menière's disease.

The second publication added state (5) where a patient standing on the force platform had some diagnosed inner ear disease. The actual diagnosis was considered irrelevant.

In the third publication the states (1) and (2) were used, but this time the measurements were done using a magnetic tracking device.

The fourth publication added a state (6) where a person standing on a force platform was a voluntary elderly person (70.8±4.0) years old.

The fifth publication dealt with the states (3) and (6). The states are understood as equivalent to classes mentioned above.

8.1 Publication 1

In the first publication the purpose was to implement a set of hidden Markov models and explore how they apply to the human swaying data. Usually these models are applied to the data that have a certain internal form. For instance, in the case of an optical character recognition [57] all characters have their individual shapes which vary a bit depending on a writer.

No clear, visually verifiable underlying shape is present in the stabilogam signals. However, if we consider the human swaying process as a black box [41, 53] which produces different outputs from different situations, we can fit a set of models to these outputs. If these models "learn" to classify different outputs correctly, we can use these models as a set of tools which can predict the correct class of an unknown output signal.

In order to teach the models and to classify different signals, the original stabilogram signals were simplified. Successive correction movements and differences in force reactions were used as features of a single swaying process.

The simplified stabilogram signals were used to teach the models and to classify three different swaying situations.

The first test situation concerned the classification of stabilogram signals of healthy young persons. The stabilogram signals were recorded from two different situations, the eyes open and the eyes closed. The research problem in this case was: Is it possible to recognize whether a person standing on a force platform is keeping the eyes open or closed? To answer this question we tested the recognition power of hidden Markov models with two to ten hidden states. To verify that the recognition was no coincidence we applied three different crossvalidation schemes which were leave-one-out, 3-fold and 11-fold crossvalidation. This test yielded the correct mean recognition rate of 85 percent when the eyes were open and 75 percent when the eyes were closed.

The second and third test situations were quite similar to the first one. Only the state of a person standing on the force platform was different. In these tests we recorded stabilogram signals of healthy young persons and patients suffering from Menière's disease. In the second test the subjects were standing on the force platform with the eyes closed and in the third test they were exposed to a virtual stimulus which was presented through the head mounted display. The research question was: Is it possible to tell whether the person standing on the force platform is a young healthy person or a patient suffering from Menière's disease. The second test yielded the mean

recognition accuracy of 77 percent in the case of young persons and 70 percent in the case of patients. The numbers in the third test were 85 percent and 75 percent respectively. The number of subjects in this work was 66, i.e. 33 patients and 33 students.

8.2 Publication 2

The results from a quantitative research can be misleading due to the properties of a sample. To reinforce our opinion that the hidden Markov models are applicable to the human swaying data we used them on the data measured from two new subject groups. In this case we had a new group of healthy young persons and a new group of patients who were suffering from some disease causing balance disorders.

The first part of this work was quite similar to the first publication. The difference was that we used a tilting force platform instead of a stationary one. Likewise we tried to predict whether a subject on the force platform was a healthy or a patient. The recognition accuracy of the healthy was approximately 80 percent depending on the number of hidden states and the respective number for the patients was also 80 percent.

The other objective of this work was to test if a simplified feature vector sequence can yield acceptable results. To accomplish this we designed a new testing procedure. In this procedure the subjects were sitting on a chair such that their feet were resting on a force platform. In front of a subject there was a computer monitor which was used to signal the subjects to stand up when a yellow rectangle appeared on the screen.

In this test we recorded the increasing force reaction during the rising. The result from this test was a one-dimensional force signal which was normalized and shortened for training and recognition purposes. The shortening means that we searched for a maximum value of each signal and took account 20 samples before the maximum and 10 samples after the maximum. Depending on the number of hidden states the mean recognition accuracy of patients was 80 percent and that of the healthy was 70 percent. This work consisted of data from 32 students and 32 otoneurological patients.

8.3 Publication 3

In the investigation of the human postural control system the force platform is the most common measuring device. It records the COP movements accurately, but it cannot capture the movements of the head and the individual limbs. In order to explore if the movements of the head, the hip and the arms are different with the eyes open and with the eyes closed, we used a magnetic tracking device instead of a force platform. The motivation of this work was based on the assumption that a subject is moving the arms in order to get a more stable position. Therefore, we can expect that we can use the movement signals of the aforementioned body parts in the recognition of different swaying cases.

In this test we collected two measurements from each subject, one with the eyes open and another with the eyes closed. In both tests the sensors of a magnetic tracking device were attached to the wrists of the both arms, to the hip on the tail bone and to the head band which was attached on the subjects head. Due to the easy test setting (quiet undisturbed stance) the signals from all sensors were almost identical. Because of this we omitted the use of hip and hand signals. The high correlation between

signals from different sensors can be verified from publication 3. We selected the head signal because it had greatest variation among all measured signals and it was measured close to a vestibular organ.

The head signal contained *x*, (left-righ) *y* (forward-backward) and *z* (up-down) components. We decided to use the acceleration of the head as a three-dimensional feature vector signal. To remove the correlation between the *x* and *y* components we rotated the signals such that the greatest variance of the signals were aligned according to the *y* axis. This was done because the subjects were not mostly positioned exactly in the same way in the magnetic field and the largest swaying is possible in the *y* (forward-backward) direction because of the structure of the ankles.

In order to reduce the number of feature vectors we used Kalman smoothing because we wanted to find such locations from a signal where the head movement changes direction (turning points). The final feature vectors were the average head acceleration between the turning points in *x, y* and *z* directions.

A part of all sequences of the successive head accelerations were used in the training of the hidden Markov models. Another part was used to test the recognition ability of the models. In this work the mean recognition accuracy of the cases when the eyes were open was 65 percent and the number for the case when the eyes were closed was 65 percent. In this work we measured 65 students.

8.4 Publication 4

In the previous papers the data had been low pass filtered or Kalman smoothed in order to find smooth turning points for the feature extraction. In this paper the approach was different because we found out that the stabilogram signals of elderly people contain more power in high frequencies than the stabilogram signals from younger people. This can be seen from figures 1 and 2 in publication 4. In order to preserve the high frequency information we decided to omit the filtering entirely.

In this work we combined the *x*- and *y*-directional signals into two one-dimensional signals which presented the lengths and angles of successive movements. In addition, we calculated these two time series for three different stabilograms from each subject. This resulted in six time series for each subject.

To reduce the amount of data per subject we created AR-models [53, 41] for each six signals and created a feature vector which contained the coefficients of these models. After this we created an observation matrix which contained all feature vectors from elderly and young subjects. From this matrix we deleted such coefficients which had the same expected values among the groups, the young and the elderly. The deletion was done on the basis of t test. To further reduce the number of coefficients in the observation matrix we made the principal component analysis, which yielded a result where six first principal components explained 91 percent of the variance in the original coefficient set. These principal components were selected to be the feature vectors for this work.

To test the classification power of feature vectors we applied four machine learning methods to our data. These methods were a neural network, 3-nearest neighbor, Fisher's linear discriminant and Mahalanobis distance. Because the components of feature vectors were uncorrelated due to principal component analysis, the Mahalanobis distance primarily told the Euclidean distance of a vector $\mathbf{x}$ from means of the two classes $\mathbf{m}_1$ and $\mathbf{m}_2$.

Because the number of the subjects was quite small, we decided to augment the data set artificially. We added 20 additional cases to both classes. These cases were generated according to the underlying normal distributions which were approximated on the basis of the data of the young and elderly.

The classification of the young and elderly was done in two different ways. First we generated only one artificially augmented data set and run 10 000 teaching/recognition stages. Second we generated 100 artificially augmented data sets and run 100 teaching/recognition stages on each augmented data sets.

The way we created the data sets and the machine learning method used did not affect the correct classification rate considerably. However, the correct classification rate was high in almost all cases. The correct mean classification rate of the elderly was 80 percent and the recognition accuracy of the students was slightly better. The data for this publication was measured from 33 students and 33 elderly persons.

8.5 Publication 5

The method presented in publication 4 works well from the machine learning point of view. However, the feature vectors used are not easy for human interpretation. In this work we continued the recognition of young students and voluntary elderly subjects. The purpose of this publication was to seek such features from the stabilogram signals that have a physical meaning and can be used for classification purposes. The basic idea of this work was based on the differences in the power spectral densities between the young and the elderly. This observation was also made in publication 4.

We made an assumption that long movements in the stabilogram signals originate from heart beats, breathing and aptitude to get more comfortable standing position. These long movements raise the need for corrective movements which are small and reside in high frequencies.

To remove the long movements and to suppress the effect of high frequency noise we bandpass filtered the x and y components of the stabilogram signals. This preprocessing resulted in the signals which can be considered as corrective movements required in maintaining the upright stance. The final feature in this work was a single scalar, which is the summed length of all corrective movements during a measurement. To justify the use of the scalar feature mentioned above we built a linear model which tried to predict our feature by a subject's mass m, height h and product mh. This model, however, was not able to explain our feature and we could leave the mass and height variables out of our feature vector because they did not bring us additional information.

We tested our new feature with two different test setups using the k-nearest neighbor algorithm with different values of k. In the first test we tried to predict whether a young student standing on the tilting force platform was keeping the eyes open or closed. The correct recognition of eyes open situations was over 90 percent. The recognition accuracy of eyes closed situation was approximately 85 percent.

In another classification task we tried to predict whether a person standing on the force platform was a young student or an elderly person. In both cases the achieved mean recognition accuracy was 70 percent. In this test we had two different sets of data. In the first test where we predicted the state of students we had 41 subjects, which were not used in the previous publications. In the second test where we

predicted whether a person standing on the force platform is a student or an elderly person, we had 33 students and 33 elderly subjects. These subjects were the same as in publication 4.

9 Discussion

The investigation of the human postural control system is difficult. Difficulties arise from the complex connections of the system, vestibular organ, vision, proprioception and learned balance control schemes, differences between individuals, temporal differences within a subject and the measurement of a phenomenon. Also, the collection of a representative data set can be problematic. Usually the healthy voluntary subjects are easy to find, but patients and persons who have balance problems may sometimes be unwilling to attend the balance tests. In addition, the measurement of patients requires an approval from an ethical committee.

The complex connections in the postural control system and the measurement of the phenomenon are closely connected. We can measure the motor control output of the balance system, but we have no access to the interaction of the vestibular organ and brain stem. This efficiently prohibits our attempt to build a model which would be able to model the function of the whole balance system. Because of this restriction we have to approach the problem by studying only the motor output.

The measurement of the motor output raises its own problems. The use of a static force platform does not allow an exhaustive balance testing. Usually the tests which can be performed with this device are too easy and they do not give us information about the situations where a subject is about to lose the balance. A tilting platform allows us to design a bit more demanding testing procedures. However, it lacks the possibility to study the balance during walking and running. According to our knowledge, the development of such a dynamic measurement system is in a quite early stage.

The different strategies between individuals to maintain balance set difficulties in the selection of useful features which could be used to characterize the swaying processes. For instance, one might say that the swaying velocity could be a good feature. In reality one person can sway a lot, but he or she does not lose balance easily whereas another person sways only a bit but loses his or her balance under a very slight external disturbance.

The ability to maintain balance can also vary within an individual. The difference is quite clear when a subject is rested or tired [22]. Also, aging affects the balance of an individual. The effect of aging to the postural system should also be studied thoroughly. The research question might be “Is a change in a stabilogram signal due to aging or due to decreased physical excercise?”

Because we have no access to the internal function of the human postural control system, we must resort to the motor control outputs which are measured with two different force platforms and a magnetic tracking device. If we look at the stabilogram in figure. 4.5, we notice that the successive points are close to each other. Without the knowledge of the input to the system, motor command from the brain, we only have the output from the system (COP). This type of dependence is possible to model with AR-models, [41, 53] especially when the individual components x and y of a stabilogram are differentiated. This makes the differentiated components stationary and we can build AR-models which efficiently characterize the dynamics of

stabilogram signals. The drawback from the classification point of view is that the parameters of AR-models are not intuitive to physicians. The parameters are also sensitive to preprocessing. Signals which are preprocessed similarly start to resemble each other and their classification power can become useless. In addition, a special care should be taken in order to prevent the overfitting to occur.

Another model which does not require any input and operates only such that it generates observable outputs is a hidden Markov model. A set of different hidden Markov models were used in the recognition of stabilogram signals and they seemed to have a good recognition power. However, it is not possible to give a certain interpretation to the hidden states of Markov models. Another problem in the use of hidden Markov models is the preprocessing of stabilogram signals. If the stabilogram signals are not filtered, the lengths of the feature vector sequences increase because of the noise from measurement devices and environment will be present. This applies to the features used in publications 1-3. On the other hand, if the stabilogram signals are "polished" too much, some of their information content is lost. Against this background it could be useful to test and compare different preprocessing methods and their impact on recognition accuracy.

For the future work we plan to augment our measurement protocol with computer vision and ENG. These techniques would better capture body movements, give additional information of the state of vestibular system and their combination features could predict the state of a subject more accurately than before. This approach also enables us the possibility to study walking subjects and maybe abandon static and tilting force platforms. This could also give us a freedom to further investigate the effect of proprioception [65] and the simulation of motor output signals [64].

One of the future challenges will also be the data collection from patients who have serious balance problems. With more data and more information we hope to get even better results than presented in the thesis. The ultimate goal is to test whether the swaying processes are different among patients suffering from different diseases. In other words, our final aim will be to predict the class of a disease on the basis of signals measured from patients.

The test in publication 3 did not use the full potential of the magnetic tracking device, because the movements of the subjects were small. One of the future tasks could be to plan a more demanding test where a subject is forced to use the arms in postural controlling tasks. Also, larger movements of the hip and the head could reveal more about the strategy of maintaining the balance.

An interesting future research would also be the comparison of different features obtained from stabilogram signals. The comparison could take into account the recognition power and interpretability of the features for human beings.

10 Conclusion

Diagnosing of diseases which cause vertigo and balance problems is really challenging. One reason for this is that vertigo is relatively infrequent and the physicians cannot build a routine for diagnosing it. Because of this an expert system ONE [3] was built to work as a support of a physician in diagnosing procedure. Such a system can also be used as a simulator when a student starts to train his or her clinical skills. However, ONE does not include the balance measurements in its current version.

Because the patients, who suffer from vertigo, have usually balance disorders a method to verify them is needed. According to the knowledge of the author, research concerning the prediction of the class of unknown stabilogram signals in not done before in large extent. In this thesis five papers address this problem. The result is that we have a set of tools which can predict the state of a subject standing on the force platform. Depending on the case the prediction accuracy is approximately 70 to 85 percent, which is good because all the subjects tested were able to walk without any problems, i.e. no one had a serious balance deficiency to distinguish those cases from the healthy during normal standing and walking. Thus, the methods and features presented in this thesis can give valuable additional information for an existing expert system.

11 Personal contributions

Publication 1

The idea came from the author of this thesis. Also, the implementation of Hidden Markov Matlab scripts as well as conducting the tests belongs to the work of the author. This publication was mainly written by Professor Martti Juhola.

Publication 2

The idea, implementation and test results were the work of the author. This paper was coauthored by Professor Martti Juhola.

Publication 3

The idea, measurements, implementation of Kalman filters and test results belong to the work of the author. Programming of the Nest of Birds interface was done by Timo Tossavainen. This paper was primarily written by Professor Martti Juhola and partially by the author.

Publication 4

Publication 4 was prepared by the author. The measurements of the elderly were done by Eeva Tuunainen.

Publication 5

Publication 5 was implemented and written by the author. The measurements of the elderly were done by Eeva Tuunainen.

12 References

1. Aalto H. Force platform posturography methodological aspects and practical applications, Academic Dissertation, Physics, University of Helsinki, Finland, 1997.

2. Arora S., Barak B. Computational complexity a modern approach, Cambridge University Press, New York, 2009.

3. Auramo Y. Construction of an expert system to support otoneurological vertigo diagnosis, Academic Dissertation, Computer Science, University of Tampere, 1999.

4. Azerro J., Schaumburg H., Spencer P. Structure and function of the somatosensory system: A neurotoxicological perspective. *Environmental Health Perspectives*, 1982, 44, pp.23-30.

5. Baloh R., Honrubia V. Clinical Neurophysiology of the vestibular system, F.A. Davis Company, USA, 1979.

6. Barber H., Stockwell C. Manual of electronystagmography, Second Edition, Mosby, St. Louis, 1980.

7. Bishop C. Neural networks for pattern recognition, Oxford University Press, New York, 1995.

8. Black F., Wall C., Rockette H., Kitch R. Normal subject postural sway during the Romberg test, American *Journal of Otolaryngology*, 3(5), 1982, pp. 309-318.

9. Bonnet S., Couturier P., Favre-Reguillon F., Guillemaud R. Evaluation of postural stability by means of a single inertial sensor, *IEEE 26th IEMBS*, San Francisco, 2004, pp. 2275-2278.

10. Brandt T. Vertigo its multisensory syndromes, Second Edition, Springer-Verlag, New York, 2000.

11. Bunke H., Caelli T. Hidden Markov models applications in computer vision, World Scientific Publishing, Singapore, 2001.

12. Calder C., Smith S. Biomechanical force-platform design based on strain gages, *Experimental Techniques*, 11, 2008, pp. 22-24.

13. Cappé O., Moulines E., Rydén E. Inference in hidden Markov models, Springer, New York, 2005.

14. Carrick F., Oggero E., Pagnacco G. Posturographic changes associated with music listening, *The Journal of Alternative and Complementary Medicine*, 13(5), 2007, 519-526.

15. Collins J., Luca C. Open-loop and closed- loop control of posture: a random-walk analysis of center-of-pressure trajectories, *Experimental Brain Research*, 95(2), 1993, pp. 303-318.

16. Conte A., Caruso G., Mora R. Static and dynamic posturography in prevalent laterally directed whiplash injuries, *European Archives of Oto-Rhino-Laryngology*, 245(4), 2004, pp. 186-192.

17. Cosman P., Cregan P., Martin C., Cartmill J. Virtual reality simulators: current status in acquisition and assessment of surgical skills, *ANZ Journal of Surgery*, 72(1), 2002, pp. 30-34.

18. Dault M., Geurts A., Mulder T., Duysens J. Postural control and cognitive task performance in healthy participants while balancing on different support-surface configurations, *Gait & Posture*, 14(3), 2001, pp. 248-255.

19. Duda R., Hart P., Stork D. Pattern classification, Second Edition, John Wiley & Sons, Canada, 2001.

20. Durbin J., Koopman S. Time series analysis by state space methods, Oxford University Press, USA, 2002.

21. Flis K., Peplowski P. Identification of human postural sway, *Open Systems & Information Dynamics*, 7(2), 2004, pp. 187-200.

22. Forsman P. Quantifying time awake posturographically, Academic Dissertation, Physics, University of Helsinki, Finland, https://oa.doria.fi/handle/10024/39285, checked, 11.5.2009.

23. Fransson P., Magnusson M., Johansson R. Analysis of adaptation in anteroposterior dynamics of human postural control, *Gait & Posture*, 7(1), 1998, pp. 64-74.

24. Fukuoka Y., Nagata T., Ishida A., Minamitani H. Characteristics of somatosensory feedback in postural control during standing. *IEEE Transactions on Neural Systems and Rehabilitation Engineering*, 2001, 9, pp. 145-153.

25. Goebel J., Hanson J., Langhofer L., Fishel D. Head-shake vestibulo-ocular reflex testing; comparison of results with rotational chair testing. *Otolaryngology- head and neck surgery*, 1994, 112, pp. 203-209.

26. Gonzales R., Woods R. Digital image processing, second edition, Prentice Hall, New Jersey, 2002.

27. Gribble P., Hertel J., Denegar C., Buckley W. The effects of fatigue and chronic ankle instability on dynamic postural control, *Journal of Athletic Training*, 39, 2004, pp. 321-329.

28. Guyon I., Gunn S., Nikravesh M., Zadeth L. Feature extraction, foundations and applications, Physica-Verlag, Springer, Netherlands, 2006.

29. Hadjikhani N., Tootell R. Projection of rods and cones within human visual cortex. *Human Brain Mapping*, 2000, 9, pp. 55-63.

30. Havia M. Menière's disease prevalence and clinical picture, Academic Dissertation, Medicine, University of Helsinki, Helsinki, Finland, 2004.

31. Haykin S. Neural networks a comprehensive foundation, Second edition, Prentice Hall, New Jersey, 1999.

32. Heiden T., Sanderson D., Inglis T., Siegmund G.. Adaptations to normal human gait on potentially slippery surfaces: the effects of awareness and prior slip experience. *Gait & Posture* 2005, 24, pp. 237-246.

33. Hill F., Kelley S. Computer graphics using OpenGL, 3rd Edition, Prentice Hall, New York, 2007.

34. Hof L. The Equations of motion for a standing human reveal three mechanisms for balance. *Journal of Biomechanics*, 40(2), 2007, pp. 451-457.

35. Hollman J., Brey R., Robb R., Bang T., Kaufman K. Spatiotemporal gait deviations in virtual reality environment, *Gait & Posture*, 23, 2006, pp. 441-444.

36. http://msdn.microsoft.com/en-us/directx/default.aspx, checked 19.5.2009.

37. http://www.5dt.com/downloads/3rdparty/nestofbirds.pdf, checked 4.5.2009.

38. http://www.datatranslation.com/products/dataacquisition/usb/dt9800.asp, checked 8.5.2008.

39. http://www.intersense.com/InertiaCube_Sensors.aspx, checked, 11.5.2009.

40. http://www.libsdl.org/, checked 8.5.2009.

41. http://www.mathworks.com/products/sysid/, checked 20.5.2009.

42. http://www.virtualresearch.com/, checked 8.5.2009.

43. Hyvärinen A., Karhunen J., Oja E. Independent component analysis, John Wiley & Sons, Canada, 2001.

44. Ito M. Cerebellar control of the vestibiulo-ocular reflex around the flocculus hyphotesis. *Annual Review of Neuroscience*, 1982, 5, pp. 275-297.

45. Jackson P. Introduction to expert systems, Addison-Wesley Longman Publishing Co., Third Edition, Boston, 1999.

46. Jacobson G., Kartush J., Newman C. Handbook of balance function testing, Singular Press, San Diego, 1997.

47. Jolliffe I. Principal Component Analysis, Second Edition, Springer-Verlag, New York, 2002.

48. Katz J. Handbook of clinical audiology, Lippnicott, Williams and Wilkins 5th Revised Edition, Baltimore, 2001.

49. Kehsner E., Kenyon R. Using immersive technology for postural research and rehabilitation, *Assistive Technology*, 16, 2004, pp. 54-62.

50. Kilburn K., Warshaw R., Hanscom B. Are hearing loss and balance dysfunction linked in construction iron workers? *Occupational and Environmental Medicine*, 1992, 49, pp.138-141.

51. Kuo A. An optimal state estimation model of a sensory integration in human postural balance, *Journal of Neural Engineering*, 2(3), 2005, pp. 235-249.

52. Liao K., Walker M., Joshi A., Reschke M., Wang Z., Leigh R. A reinterpretation of the purpose of the translational vestibulo-ocular reflex in human subjects. *Progress in Brain Research*, 2008, 171, pp. 295-302.

53. Ljung L. System identification theory for the user, Second Edition, Prentice Hall, New York, 1999.

54. Looney C. Pattern recognition using neural networks theory and algorithms for engineers and scientists, Oxford University Press, New York, 1997.

55. Luna F. Introduction to 3D game programming with DirectX 9.0, Wordware Publishing, Inc. Texas, 2003.

56. Mahboobin A., Beck C., Moeinzadeh M., Louglhlin P. Analysis and validation of a postural control model, *American Control Conference*, 5, 2002, Anchorage, 4122-4128.

57. Mantas J. An overview of character recognition methodologies, *Pattern Recognition*, 19(6), 1986, pp. 425-430.

58. Matthews J., Howell R. Complex analysis for mathematics and engineering, Fifth Edition, Jones and Bartlett Publishers Inc. London, 2006.

59. Mitra S. Digital signal processing, a computer based approach, Third Edition, McGraw-Hill, New York, 2006.

60. Montgomery D., Peck E., Vining G. Introduction to linear regression analysis, Third Edition, Wiley & Sons, Canada, 2001.

61. Oppenheimer A. Schafer R. Digital Signal Processing, Prentice Hall, Englewood Cliffs, New Jersey, 1975.

62. Pausch R., Proffit D., Williams G.. Quantifying immersion in virtual reality, *Proceedings in 24th Annual Conference on Computer Graphics and Interactive Techniques*, Los Angeles, 1997, pp. 13-18.

63. Rabiner R.. A tutorial on hidden Markov models and selected applications in speech recognition, *Proceedings of IEEE* 77, pp. 257-285, 1989.

64. Rasku J., Juhola M. Classification of task driven swaying paths, *21st IEEE International Symposium on Computer-Based Medical Systems*, Jyväskylä, Finland, 2008, pp. 284-286.

65. Rasku J., Juhola M., Pyykkö I., Toppila E., Varpa K. The effect of removing the force feedback during the quiet stance, accepted to *MIE2009*, Bosnia Herzegovina, Sarajevo 2009.

66. Reid A., Marchbanks R., Ernst A. Intracranial and inner ear physiology and pathophysiology, Whurr Publishers Ltd, London, 1998.

67. Ripley B. Pattern recognition and neural networks, Cambridge University Press, United Kingdom, 1996.

68. Rosenberg L. The effect of interocular distance upon operator performance using stereoscopic displays to perform virtual depth tasks, *IEEE Virtual Reality Annual International Symposium*, Seattle, 1993, pp. 27-32.

69. Selmani Z. Otoneurological work-up in Meniére's disease and other inner ear disorders, Academic Dissertation, Medicine, University of Tampere, Finland, 2004.

70. Shreiner D., Woo M., Neider J., Davis T. OpenGL programming guide, Sixth Edition, Addision-Wesley, New York, 2008.

71. Smith S. The scientist & engineer's guide to digital signal processing, California Technical Publishing, San Diego, 1997.

72. Soechting J., Bertzhoz A. Dynamic role of vision in the control of posture in man, *Experimental Brain Research*, 36(3), 1978, pp. 551-561.

73. Theodoridis S., Koutroumbas K. Pattern recognition, Third Edition, Elsevier, USA, 2006.

74. Toppila E. A systems approach to individual hearing conservation, Academic Dissertation, Physics, University of Helsinki, Finnish Institute of Occupational Health, Helsinki, Finland, 2000.

75. Tossavainen T. Feature subset selection for a diagnostic test of human balance, *European Notes in Medical Informatics*, *MIE2005*, Switzerland, 2005, pp. 1117-1122.

76. Tossavainen T. Virtual reality and posturography applied to postural control research, Academic Dissertation, Computer Science, University of Tampere, Finland, 2006.

77. Tossavainen T., Juhola M., Pyykkö I., Aalto H., Toppila E. Development of virtual reality stimuli for force platform posturography, *International Journal of Medical Informatics*, 70, 2003, pp. 277-283.

78. Tossavainen T., Juhola M., Pyykkö I., Toppila E., Aalto H., Honkavaara P. Towards virtual reality stimulation in force platform posturography, *Proceedings*

of the 10th World Congress on Medical Informatics, Amsterdam, 2001, pp. 854-857.

79. Tossavainen T., Toppila E., Pyykkö I., Forsman P., Juhola M., Stark J. Virtual Reality in Posturography, *IEEE Transactions on Information Technology in Biomedicine*, 2005, pp. 1-11.

80. Trächtler M., Hodgins D., Kenney L., Dienger M., Link T., Manoli Y. Multi-axis inertial measurement units measuring human posture and motion, *IFMB Proceedings*, RWTH Aachen University, Germany, 13, 2007, pp. 184-188.

81. Tyler A. Expert systems research trends, Nova Science Publishers, New York, 2007.

82. Uimonen S., Sorri M., Laitakari K., Jämsä T. A comparison of three vibrators in static posturography: the effect of vibration amplitude on body sway, *Medical Engineering and Physics*, 18, 1996, pp. 405-409.

83. Van Daele U., Huyvaert S., Hagman F., Duguet W., Van Gheluwe B., Vaes P. Reproducibility of postural control measurement during unstable sitting in low back pain patients, *BMC Musculoskeletal Disorders*, 8, 2007, Online access.

84. Vouriot A., Hannhart B., Gauchard G., Barot A., Ledin T., Mur J., Perrin P. Long-term exposure to solvents impairs vigilance and postural control in serigraphy workers. *Occupational and Environmental Health*, 2005, 78, pp. 510-515.

85. Webb A. Statistical pattern recognition, Second Edition, John Wiley & Sons, West Sussex, 2007.

86. Welch G., Bishop G. An introduction to Kalman filters, *ACM Siggraph* Course 8, Los Angeles, 2001.

87. Wellas B., Wayne S., Romero L., Baumgartner R, Garry P. Fear of falling and restriction of mobility in elderly fallers. *Age and Ageing*, 1997, 26, pp. 189-193.

88. Winter D. Human balance and posture control during standing and walking, *Gait & Posture*, 3(4), 1995, pp.193-214.

89. Yokoyama K., Araki S., Nishikitani M., Sato H. Computerized posturography with sway frequency analysis: application in occupational and environmental health, *Industrial Health*, 40, 2002, pp. 14-22.

Publication I

Modelling stabilograms with hidden Markov models

Jyrki Rasku, Martti Juhola, Timo Tossavainen, Ilmari Pyykkö, Esko Toppila

Publication II

Recognition of balance signals between healthy students and otoneurological patients with hidden Markov models

Jyrki Rasku, Martti Juhola, Esko Toppila, Ilmari Pyykkö

Publication III

A detection method of body movement signals measured with magnetic tracking device for human balance investigations

Jyrki Rasku, Martti Juhola

Publication IV

Looking for differences in postural control systems: young students versus pensioners

Jyrki Rasku, Martti Juhola

Publication V

A method for the classification of corrective activity in context dependent postural controlling tasks

Jyrki Rasku